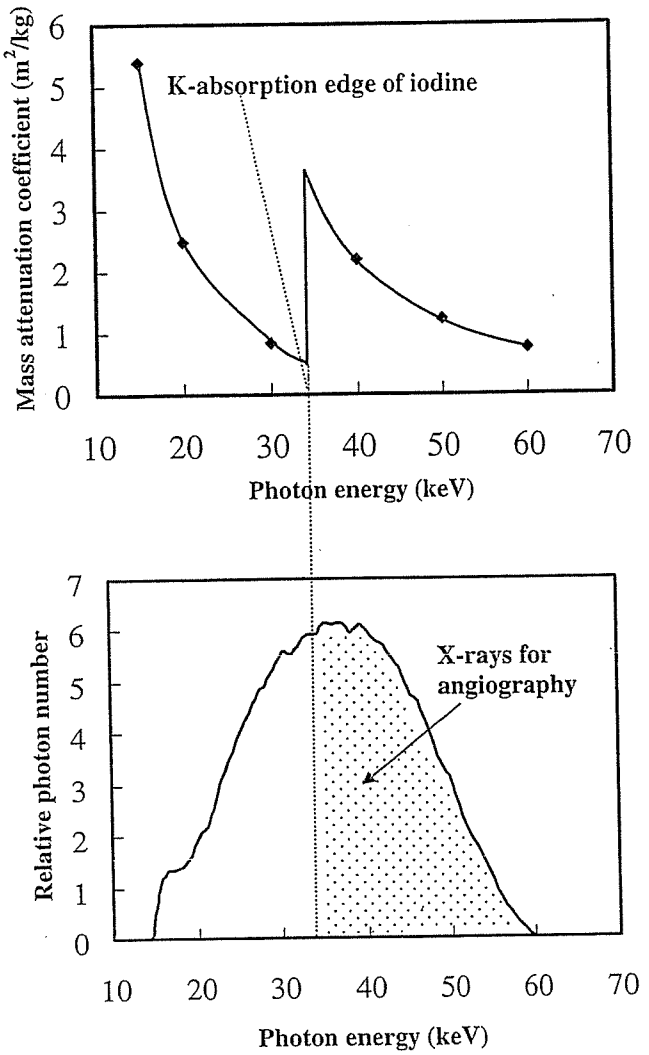

Fig. 1. Mass attenuation coefficients of iodine and bremsstrahlung X-rays for enhanced K-edge angiography.

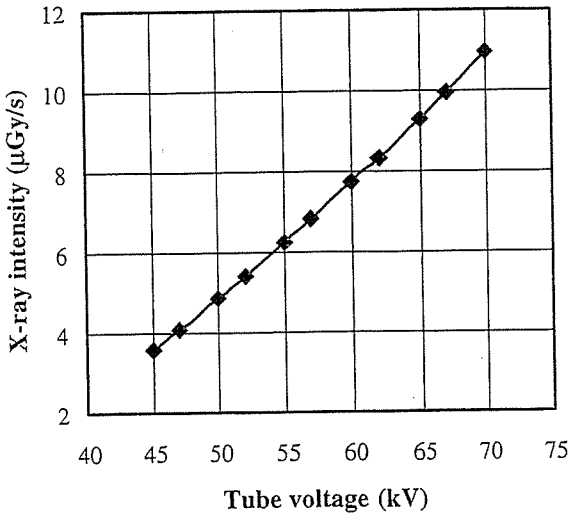

Fig. 2. X-ray intensity (μGy/s) as a function of tube voltage (kV) with tube current of 100 μA.

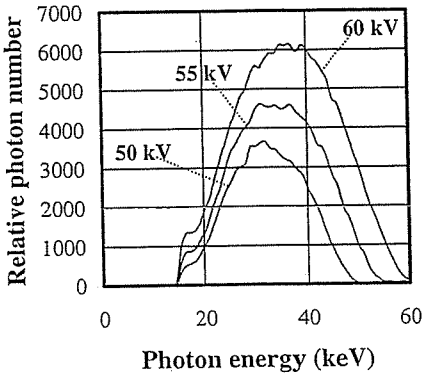

Fig. 3. Bremsstrahlung X-ray spectra measured using cadmium telluride detector with changes in tube voltage.

respectively. The focal-spot size was proportional to the electric power of the tube, and its size was approximately 20 μm in diameter with a power of 20 W. In this experiment, the tube voltage applied ranged from 45 to 70 kV, and the tube current was regulated to within 170 μA. The exposure time is controlled to obtain optimum X-ray intensity for angiography, and narrow-photon-energy bremsstrahlung X-rays are produced using the aluminum filter.

4. Results

4.1 X-ray intensity

X-ray intensity was measured using a Victoreen 660 ionization chamber, with a volume of 400 cm^3, at 1.0 m from the X-ray source using the filter (Fig. 2). At a constant tube current of 100 μA, X-ray intensity increased when tube voltage was increased. At a tube voltage of 60 kV, the X-ray intensity with the filter was 7.75 μGy/s.

4.2 X-ray spectra

To measure X-ray spectra using the filter, we employed a cadmium telluride detector (CDTE2020X, Hamamatsu Photonics) (Fig. 3). When tube voltage was increased, bremsstrahlung X-ray intensity increased, and both maximum photon energy and spectrum peak energy increased.

To perform K-edge angiography, bremsstrahlung X-rays of approximately 35 keV are used; the high-energy bremsstrahlung X-rays decrease image contrast. When this filter was used, because bremsstrahlung X-rays with energies higher than 60 keV were not absorbed easily, the tube voltage for angiography was determined to be 60 kV by considering the filtering effect of radiographic objects.

4.3 Enhanced magnification angiography

The enhanced angiography was performed by fourfold magnification imaging using the CR system and the filter at a tube voltage of 60 kV, and the distance between the X-ray source and the imaging plate was 1.0 m (Fig. 4). First, the spatial resolutions of cohesion and magnification radiographies were realized using a lead test chart at an exposure time of 30 s. In the magnification radiography, 50-μm-thick lines (10 line pairs) were clearly visible (Fig. 5). Figure 6 shows radiograms of tungsten wires in a 25-mm-diameter rod made of poly(methyl methacrylate) (PMMA) at an exposure time of 30 s. Although image contrast decreased slightly with decreasing wire diameter owing to the blurring of the image caused by the sampling pitch of 87.5 μm, a 20-μm-diameter wire could be observed.

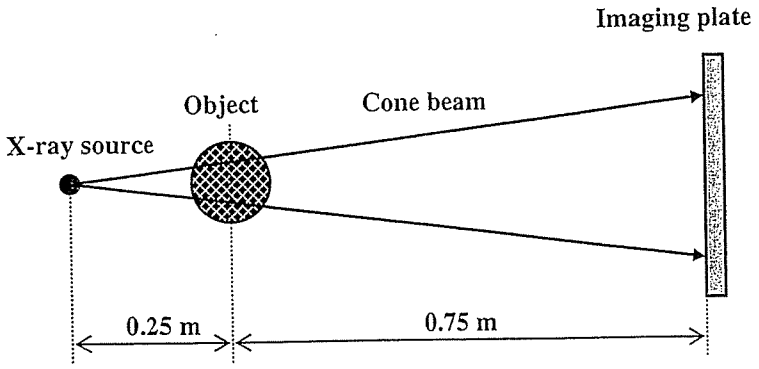

Fig. 4. Fourfold magnification imaging using imaging plate in conjunction with microfocus tube.

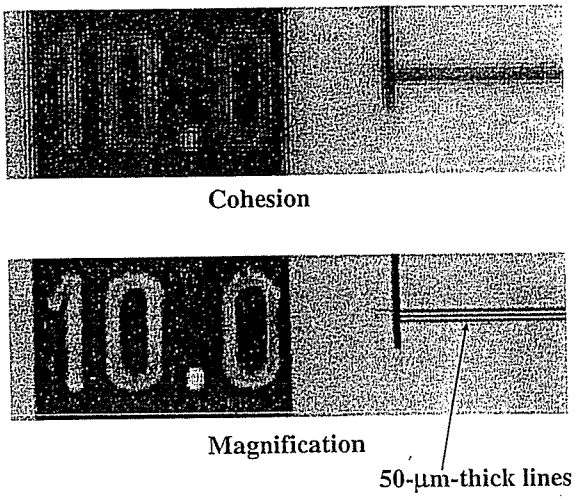

Fig. 5. Radiogram of test chart for measuring spatial resolution.

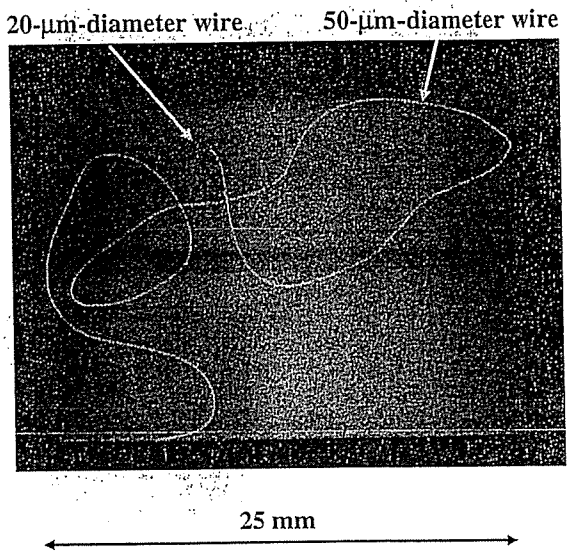

Fig. 6. Radiograms of tungsten wires in PMMA rod.

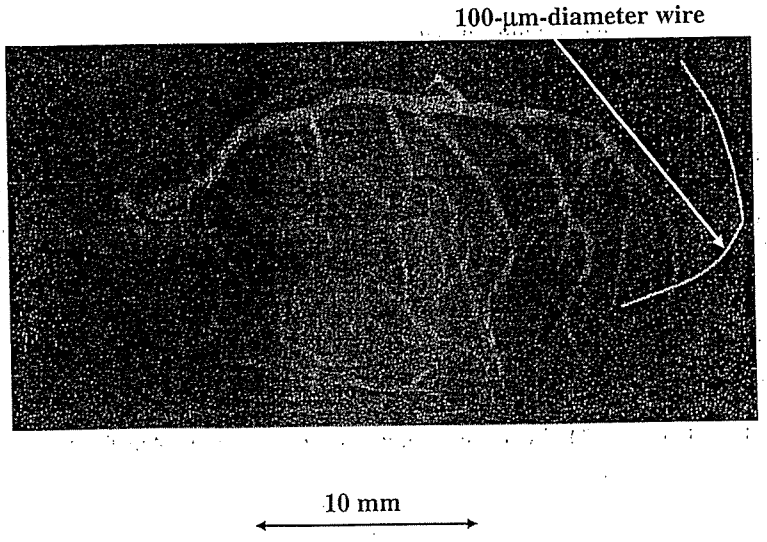

Fig. 7. Angiogram of extracted rabbit heart using iodine microspheres.

Figures 7 and 8 show angiograms of a 19-mm-thick rabbit heart specimen and a 41-mm-thick thigh specimen, respectively. The exposure time was 30 s, and these images were obtained using iodine microspheres of 15 μm diameter. The microspheres are very useful for making the phantoms of nonliving animals used for angiography. The iodine plastic spheres contained 37% iodine by weight, and the coronary arteries and fine blood vessels were visible.

Figure 9 shows angiograms of a dog heart specimen of 65 mm thickness using iodine spheres with an exposure time of 60 s. Although the image contrast decreased slightly with increasing thickness of the PMMA plate facing the X-ray

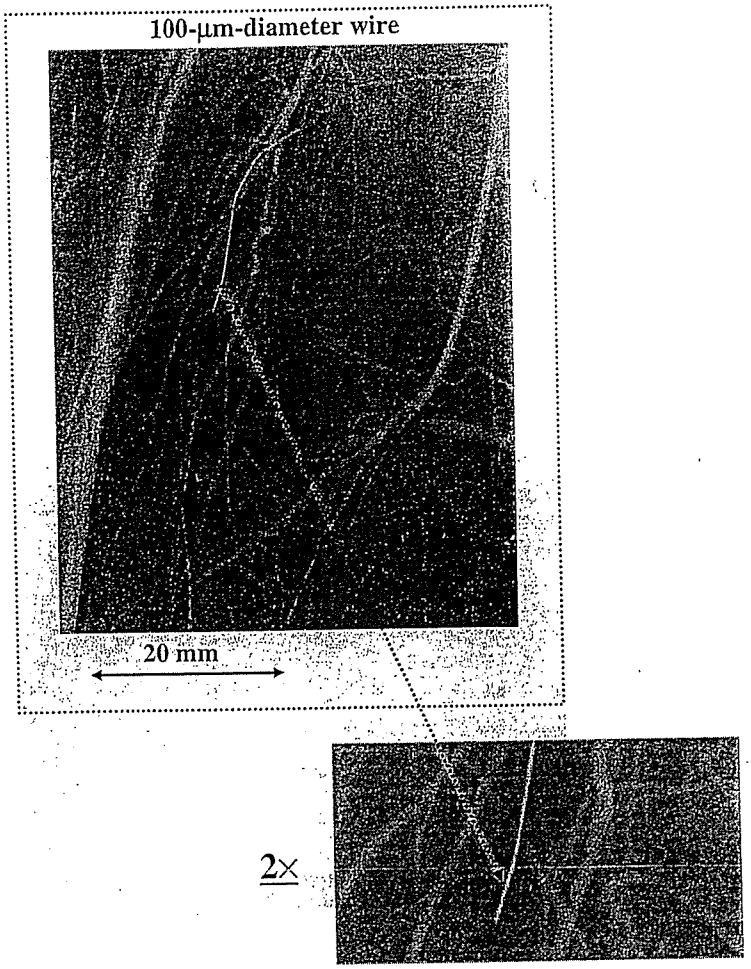

Fig. 8. Angiograms of rabbit thigh.

source, the coronary arteries of approximately 100 μm diameter were observed using a 100-mm-thick plate.

5. Conclusions

We employed a microfocus X-ray generator with a tungsten target tube to perform enhanced magnification angiography using narrow-photon-energy bremsstrahlung X-rays at a peak photon energy of approximately 38 keV, which can be absorbed easily by iodine-based contrast media. Although bremsstrahlung X-ray intensity substantially increased with increasing tube voltage, the optimal tube voltage for increasing image contrast was determined to be 60 kV.

Because the sampling pitch of the CR system is 87.5 μm, we obtained spatial resolutions of approximately 50 μm using fourfold magnification imaging achieved with a 20-μm-focus tube. To observe fine blood vessels of less than 100 μm diameter, the spatial resolution of the CR system should be improved to 43.8 μm (Regius 190, Konica Minolta), and iodine density should be increased.

In this research, we controlled bremsstrahlung X-rays to the optimum spectral distribution for realizing enhanced angiography using iodine-based contrast media. On the other hand, gadolinium-based contrast media with a K-edge energy of 50.2 keV have been employed to perform angiography in MRI, and the gadolinium density used has been increasing. In view of this situation, tungsten Kα rays (58.9 keV) are useful for enhancing K-edge angiography, because the Kα rays are absorbed effectively by gadolinium media. As compared with angiography using iodine media, the absorbed dose can be decreased considerably using gadolinium media.

At a tube voltage of 60 kV and a current of 170 μA, the photon number was approximately 2×10^7 photons/(cm^2·s) at 1.0 m from the source, and photon count rate can be increased easily using a rotating anode microfocus tube developed by Hitachi Medical Corporation. Recently, the maximum electric power of the microfocus X-ray tube has been increasing, and a kilowatt-range tube is realizable. Therefore, real-time magnification radiography will become possible using a flat panel detector with a pixel size of less than 100 μm.

Acknowledgments

This work was supported by Grants-in-Aid for Scientific Research (13470154, 13877114, and 16591222) and Advanced Medical Scientific Research from MECSST, Health and Labor Sciences Research Grants (RAMT-nano-001, RHGTEFB-genome-005 and RHGTEFB-saisei-003), and grants from the Keiryo Research Foundation, Promotion and Mutual Aid Corporation for Private Schools of Japan, Japan Science and Technology Agency (JST), and New Energy and Industrial Technology Development Organization (NEDO, Industrial Technology Research Grant Program in '03).

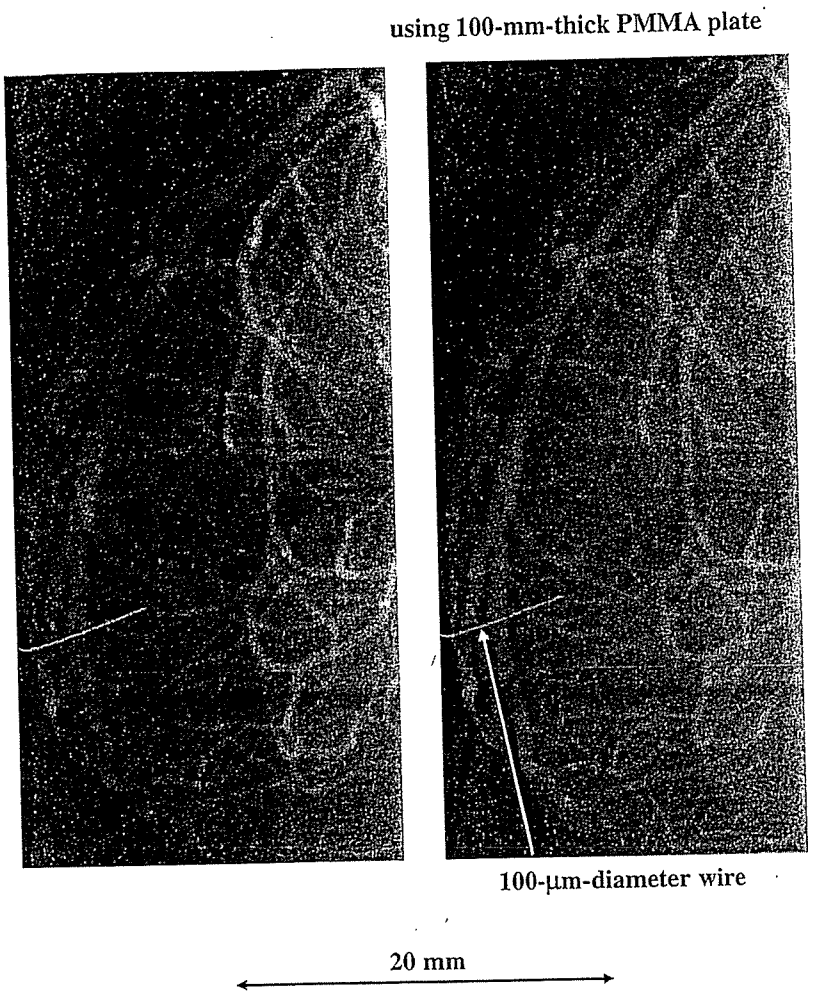

Fig. 9. Angiograms of extracted dog heart.

1) E. Sato, S. Kimura, S. Kawasaki, H. Isobe, K. Takahashi, Y. Tamakawa and T. Yanagisawa: Rev. Sci. Instrum. **61** (1990) 2343.
2) K. Takahashi, E. Sato, M. Sagae, T. Oizumi, Y. Tamakawa and T. Yanagisawa: Jpn. J. Appl. Phys. **33** (1994) 4146.
3) E. Sato, K. Takahashi, M. Sagae, S. Kimura, T. Oizumi, Y. Hayasi, Y. Tamakawa and T. Yanagisawa: Med. Biol. Eng. Comput. **32** (1994) 289.
4) E. Sato, M. Sagae, K. Takahashi, A. Shikoda, T. Oizumi, Y. Hayasi, Y. Tamakawa and T. Yanagisawa: Med. Biol. Eng. Comput. **32** (1994) 295.
5) E. Sato, Y. Hayasi, R. Germer, E. Tanaka, H. Mori, T. Kawai, T. Ichimaru, K. Takayama and H. Ido: Rev. Sci. Instrum. **74** (2003) 5236.
6) E. Sato, Y. Hayasi, R. Germer, E. Tanaka, H. Mori, T. Kawai, T. Ichimaru, S. Sato, K. Takayama and H. Ido: J. Electron Spectrosc. Relat. Phenom. **137–140** (2004) 713.
7) E. Sato, E. Tanaka, H. Mori, T. Kawai, S. Sato and K. Takayama: Opt. Eng. **44** (2005) 049002.
8) E. Sato, M. Sagae, E. Tanaka, Y. Hayasi, R. Germer, H. Mori, T. Kawai, T. Ichimaru, S. Sato, K. Takayama and H. Ido: Jpn. J. Appl. Phys. **43** (2004) 7324.
9) E. Sato, E. Tanaka, H. Mori, T. Kawai, T. Ichimaru, S. Sato, K. Takayama and H. Ido: Med. Phys. **32** (2005) 49.
10) E. Sato, Y. Hayasi, K. Kimura, E. Tanaka, H. Mori, T. Kawai, T. Inoue, A. Ogawa, S. Sato, K. Takayama, J. Onagawa and H. Ido: Jpn. J. Appl. Phys. **44** (2005) 8716.
11) A. Momose, T. Takeda, Y. Itai and K. Hirano: Nat. Med. **2** (1996) 473.
12) M. Ando, A. Maksimenko, H. Sugiyama, W. Pattanasiriwisawa, K. Hyodo and C. Uyama: Jpn. J. Appl. Phys. **41** (2002) L1016.
13) H. Mori, K. Hyodo, E. Tanaka, M. U. Mohammed, A. Yamakawa, Y. Shinozaki, H. Nakazawa, Y. Tanaka, T. Sekka, Y. Iwata, S. Honda, K. Umetani, H. Ueki, T. Yokoyama, K. Tanioka, M. Kubota, H. Hosaka, N. Ishizawa and M. Ando: Radiology **201** (1996) 173.
14) K. Hyodo, M. Ando, Y. Oku, S. Yamamoto, T. Takeda, Y. Itai, S. Ohtsuka, Y. Sugishita and J. Tada: J. Synchrotron Radiat. **5** (1998) 1123.
15) S. W. Wilkins, T. E. Gureyev, D. Gao, A. Pogany and A. W. Stevenson: Nature **384** (1996) 335.
16) A. Ishisaka, H. Ohara and C. Honda: Opt. Rev. **7** (2000) 566.
17) E. Sato, K. Sato and Y. Tamakawa: Annu. Rep. Iwate Med. Univ. School Liberal Arts Sci. **35** (2000) 13.
18) E. Sato, E. Tanaka, H. Mori, T. Kawai, T. Ichimaru, S. Sato, K. Takayama and H. Ido: Med. Phys. **31** (2004) 3017.
19) E. Sato, E. Tanaka, H. Mori, T. Kawai, T. Inoue, A. Ogawa, A. Yamadera, S. Sato, F. Ito, K. Takayama, J. Onagawa and H. Ido: Jpn. J. Appl. Phys. **44** (2005) 8204.
20) A. B. Crummy, C. A. Mistretta, M. G. Ort, F. Kelcz, J. R. Cameron and M. P. Siedband: Radiology **8** (1973) 402.
21) R. A. Kruger, C. A. Mistretta, A. B. Crummy, J. F. Sackett, M. M. Goodsit, S. J. Riederer, T. L. Houk, C. G. Shaw and D. Flemming: Radiology **125** (1977) 234.
22) F. Kelcz and C. A. Mistretta: Med. Phys. **3** (1977) 159.

Tokai J Exp Clin Med., Vol. 31, No. 2, pp. 49-52, 2006

Efficient Preparation of Cationized Gelatin for Gene Transduction

Naoto FUKUYAMA, Tsuyoshi ONUMA[*1], Shio JUJO, Yoshifumi TAMAI[*2], Takahiro SUZUKI[*3], Kazunori MYOJIN[*4], Yasuhiko TABATA[*5], Yoshimi ISHIHARA[*1], Jiro TAKANO[*1] and Hidezo MORI[*6]

*Department of Physiology, [*2] Department of Radiation Oncology,*
*[*3] Department of Ophthalmology, [*4] Department of Radiology, Tokai University School of Science*
*[*1] Department of Chemistry, Tokai University School of Science*
*[*5] Department of Frontier Medical Sciences, Kyoto University*
*[*6] Department of Cardiac Physiology, National Cardiovascular Center*

(Received November 21, 2005; Accepted April 12, 2006)

We previously reported gene therapy using cationized gelatin microspheres of ϕ20-32 μm, prepared from pig skin, as a transducing agent, but although the gelatin offered various advantages, its yield was extremely low (only 0.1%). In this study, we markedly improved the yield of ϕ20-32 μm cationized gelatin microspheres and prepared a newly less than ϕ20 μm cationized gelatin. Conventionally, cationized gelatin is prepared by cationization, particulation by agitation, and cross-linking. The yield is determined by the particulation step, for which we had used a three-necked distillation flask of 500 mL and an agitation speed of 420 rpm. The yield was significantly increased from 0.13 ± 0.02% to 8.80 ± 1.90% by using a smaller flask of 300 mL and an agitation speed of 25000 rpm ($p < 0.01$). We could also prepare cationized gelatin of less than ϕ20 μm, which had not been possible previously. We confirmed that efficient gene introduction into peritoneal macrophages could be achieved with the new cationized gelatin.

Key words: gelatine microsphere, macrophage, yield

INTRODUCTION

Efficient gene transduction methods are necessary for gene therapy [1], and currently available methods can be divided into viral vector techniques and non-viral approaches, such as lipofection or electroporation. Viral vectors such as adenovirus or retrovirus offer high transduction efficiency, but there are questions regarding safety [2]. On the other hand, the efficiency of transduction with non-viral vectors is generally poor [3]. In recent years, nucleofection has been developed for highly efficient gene transduction, but it can be applied to only certain cells, and it causes damage in some cases [4].

We showed that intramuscular injection of FGF-4 gene-gelatin complex induced significantly greater angiogenesis than injection of the bare FGF-4 gene [5]. Furthermore, we showed that adrenomedullin (AM) gene-gelatin complex effectively transduced the AM gene into endothelial progenitor cells (EPCs), and the transduced EPCs had a therapeutic effect in pulmonary hypertension [6]. In those studies, we used cationized gelatin microspheres of ϕ20-32 μm, derived from pig skin. However, the yield of gelatin was only about 0.1%. Cascone *et al.* reported that the preparation of nanoparticulate gelatin required an agitation speed of cationized gelatin and olive oil of more than 10,000 rpm [7], so in this study, we examined whether the use of a higher agitation speed during preparation of the gelatin particles would increase the yield and reduce the particle size in our procedure. We also confirmed the efficacy of the gelatin particles thus obtained for gene transduction.

MATERIALS

Gelatin of pig skin origin (PI 9) was purchased from Nitta Gelatin Corp, Japan. 1-Ethyl-3-(3-dimethylaminopropyl) carbodiimide (EDC), β-alanine, acetone, glycine, hydrochloric acid, ethylenediamine, olive oil, glutaraldehyde solution (GA), potassium dihydrogenphosphate, disodium hydrogenphosphate and sodium hydrogen carbonate were purchased from Wako Pure Chemical Industry, Japan. Liquid nitrogen was purchased from Tomoe Corporation, Japan.

Rat peritoneal macrophages were collected by intraperitoneal injection of thioglycolate culture medium as previously described [8]. DNA encoding GFP with the cytomegalovirus enhancer-chicken β-actin hybrid promoter was constructed [5].

METHODS

Conventional preparation of gelatin microspheres involves three steps: (1) cationized gelatin production, (2) microsphere production and (3) cross-linking of cationized gelatin microspheres. In order to increase the yield of cationized gelatin microspheres, we aimed to improve the second step, i.e., microsphere production.

Cationized gelatin production

PI 9 (10 g) was completely dissolved in 0.1 M phosphate buffer (PBS, 450 mL) containing potassium dihydrogenphosphate and disodium hydrogenphosphate. Ethylenediamine (31.1 mL) and hydrochloric acid were added, and the pH was adjusted to 5.0. EDC (5.35 g) was added to this solution, which was made up to 500 mL with PBS and left for 18 hours. The solution was

Naoto FUKUYAMA or Hidezo MORI, Department of Physiology, Tokai University, Bohseidai, Isehara, Kanagawa 259-1193, Japan Tel: +81-463-931-121 Fax: +81-463-936-684 E-mail: fukuyama@is.icc.u-tokai.ac.jp

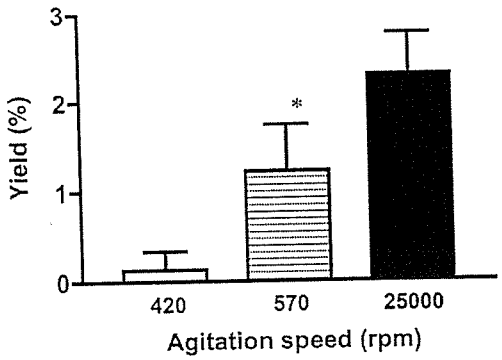

Fig. 1 Yield of ϕ20-32 μm cationized gelatin using a 500 mL three-necked distillation flask.
The open bar shows the control (420 rpm) group, horizontal lined bar, the 570 rpm group and closed bar, the 25,000 rpm group. Data are presented as mean ± SEM. The yield in the 570 rpm group was significantly higher than that in the control group (*p <0.001 vs 420 rpm).

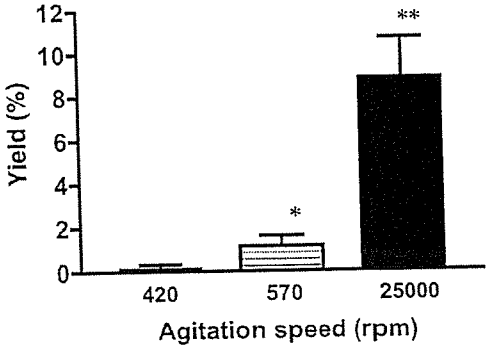

Fig. 2 Yield of ϕ20-32 μm cationized gelatin using a 300 mL three-necked distillation flask.
The open bar shows the 420 rpm group, horizontal lined bar, the 570 rpm group and closed bar, the 25,000 rpm group. Data are presented as mean ± SEM. The yield in the 570 rpm group was significantly higher than that in the 420 rpm group (*p < 0.001 vs 420 rpm). The yield in the 25,000 rpm group was significantly higher than that in the other groups (**p <0.0001 vs other groups).

then dialyzed for 2 days with 16 changes of water. After the dialysis, this solution was freeze-dried for 4 to 7 days to afford cationized gelatin. The conversion rate of carboxyl groups to amino groups was measured by the TNBS method to characterize the product [13].

Microsphere production

In the conventional procedure, cationized gelatin aqueous solution and olive oil were placed in a three-necked distillation flask of 500 mL at 40°C, and centrifuged at 420 rpm for 10 minutes. This solution was stirred for 30 minutes at 0°C. Acetone was added, and the mixture was centrifuged. After centrifugation, the oil layer was removed, and acetone was added. This solution was centrifuged again, homogenized and sieved with ϕ20 μm, ϕ32 μm and ϕ90 μm sieves (Test sieves, #JIS Z 8801, Tokyo Screen Co., Ltd., Japan). The microspheres was dried in a refrigerator overnight, and the yield of each fraction was determined.

In this experiment, we examined the effect of increasing the agitation speed to 570 rpm and 25000 rpm, and the effect of using a smaller three-necked distillation flask (300 mL) to obtain smoother mixing.

Cross-linking of cationized gelatin microspheres

Acetone and hydrochloric acid (7:3) were added to cationized gelatin microspheres, the crosslinking agent GA was added, and the reaction was allowed to proceed for 24 hours. After the reaction, centrifugation was performed and the supernatant was removed. Glycine solution (100 mM) was added to remove GA for one hour. After centrifugation, the supernatant was removed and cross-linked microspheres were cooled with liquid nitrogen, freeze-dried, and weighed.

Gene introduction with the newly developed cationized gelatin microspheres

Gene gelatin complex was prepared by mixing 2 mg of cationized gelatin and 50 μg/100 μl gene (GFP or luciferase). The complex was incubated with rat peritoneal macrophages for 14 days. Effective gene introduction was demonstrated by cellular expression of GFP or luciferase.

RESULTS

Effect of agitation conditions on yield of cationized gelatin

In the conventional method (500 mL/420 rpm), the yield of the ϕ20-32 μm cationized gelatin was 0.13 ± 0.02%, but when the agitation speed was increased to 570 rpm, the yield rose to 1.22 ± 0.52% (*p < 0.001 vs 420 rpm). The yield was further increased to 2.30 ± 0.47% by increasing the agitation speed to 25000 rpm from 570 rpm, but this further increase was not statistically significant (p=0.136)(Fig. 1). Next we used a smaller (300 mL) three-necked distillation flask with agitation at 420 rpm, 570 rpm and 25,000 rpm. When the agitation speed was increased to 570 rpm, the yield rose to 1.12 ± 0.49% from 0.11 ± 0.01% (*p <0.001 vs 420 rpm). The yield was markedly increased to 8.80 ± 1.90% by increasing the agitation speed to 25,000 rpm from 570 rpm (**p <0.0001 vs 420 or 570 rpm) (Fig. 2).

The yields of different-sized microsphere fractions are summarized in Table 1. The use of the highest agitation speed and the smaller flask allowed us to obtain cationized gelatin microspheres of less than ϕ20 μm, which we had not been able to prepare with the conventional method, in addition to increasing the total yield of the cationized gelatin microspheres.

Gene introduction with the new cationized gelatin

We examined the efficiency of the new, smaller-sized cationized microspheres for gene introduction into rat peritoneal macrophages. As shown in Figure 3A, after coincubation of the macrophages and GFP

Table 1 Yields of different-sized cationized gelatines (%).

Flask size (mL) / Agitation speed (rpm)	$> \phi 20$ μm	$\phi 20$-32 μm	$\phi 32$-90 μm	$\phi 90$ μm $>$
500/420	0	0.13±0.02	15.1±3.21	14.0±5.30
500/570	0	1.22±0.52*	13.2±3.52	14.1±6.13
500/25000	0	2.30±0.47	17.2±4.10	7.23±1.60
300/420	0	0.11±0.01	19.1±5.32	17.4±7.12
300/570	0	1.12±0.49**	22.1±7.62	11.3±2.52
300/25000	2.12±0.21	8.80±1.90***	32.2±11.0	9.10±2.10

Data are presented as mean ± SEM. *p <0.001 vs 500/420, **p <0.001 vs 300/420
***p <0.0001 vs 300/420 or 300/570

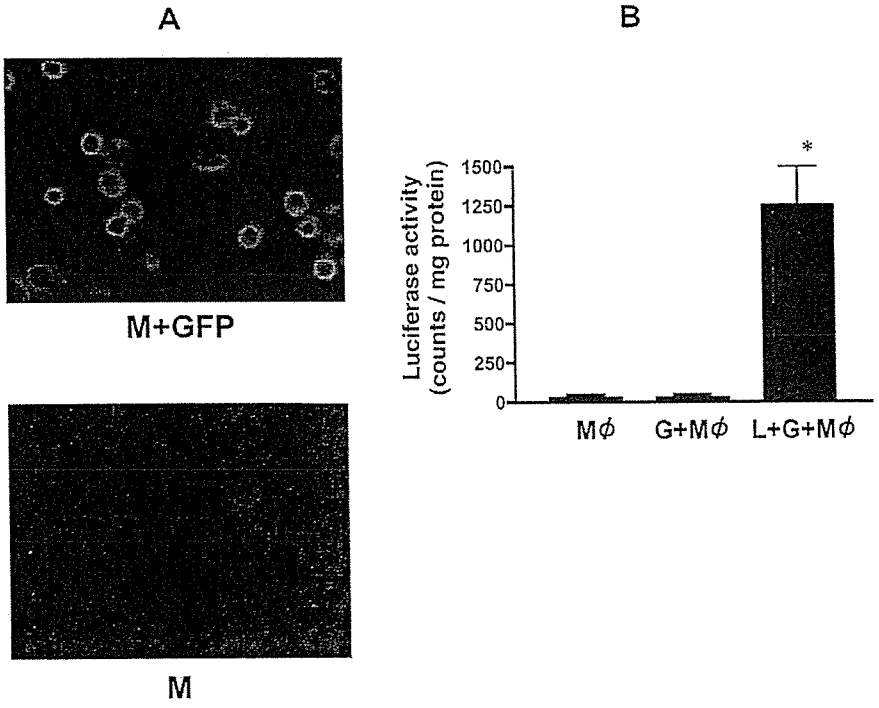

Fig. 3 Gene introduction into rat peritoneal macrophages with cationized gelatin.
A. Upper column: Peritoneal macrophages were coincubated with GFP gene-cationized gelatin complex (M + GFP) for 14 days. GFP was expressed in the cytoplasm of the macrophages. Lower column: Peritoneal macrophages were coincubated with cationized gelatin complex (M) for 14 days. GFP was not expressed in the macrophages.
B. Luciferase activity. Peritoneal macrophages were coincubated with luciferase gene-cationized gelatin complex (L + G + Mϕ, closed bar) or with cationized gelatin (G + Mϕ, horizontal lined bar) or with no additive (Mϕ, open bar) for 14 days. Data are presented as mean ± SEM. The luciferase activity of L+G+Mϕ was significantly higher than that of Mϕ or G+Mϕ (*p <0.01).

gene-cationized gelatin complex, the cells expressed GFP. Coincubation of the macrophages and cationized gelatin alone did not result in expression of GFP. As shown in Figure 3B, after coincubation of the macrophages and luciferase gene-cationized gelatin complex, the cells expressed luciferase activity of 1251 ± 257 (counts/mg protein) on day 14, while the activity in the control group, in which macrophages were cultured alone, was only 5 ± 2 (counts/mg protein) (*p <0.01). The luciferase activity was 8 ± 2 (count/mg protein) in the macrophage + cationized gelatin group.

DISCUSSION

In this study, we showed that the yield of cationized gelatin microspheres of $\phi 20$-32 μm increased with increasing agitation speed and with the use of a smaller three-necked flask for the agitation of cationized gelatin with olive oil. In addition, cationized gelatin microspheres smaller than $\phi 20$ μm could be prepared for the first time with the highest agitation speed and the smaller flask.

In the conventional method, 30% of cationized

gelatin finally formed microspheres, but almost all were larger than ϕ32 μm [9]. Gene introduction with cationized gelatin microspheres involves cellular phagocytic activity, which is inefficient for particles as large as ϕ30 μm [6]. By using a speed as high as 25,000 rpm and a smaller flask (300 mL), we were able to increase the yield of cationized gelatin microspheres of ϕ20-32 μm to 8.80%. Furthermore, we could manufacture cationized gelatin microspheres smaller than ϕ20 μm, which could not be obtained by the conventional method, in a yield of 2.12%.

Gedanken *et al.* succeeded in the production of nanoparticles from various chemicals by using ultrasonic irradiation [10]. However, when we used an ultrasonic homogenizer for agitating cationized gelatin and olive oil, the yield decreased to 1.30% .

We previously showed that our gelatin microsphere-gene complexes were introduced into cells by phagocytosis. Since the efficiency of cellular phagocytotic activity is greater for smaller particles, the development of smaller-sized cationized gelatin microspheres is expected to increase the efficiency of gene introduction via phagocytosis. Further, Kaul *et al.* showed that gene introduction into fibroblasts, which exhibit endocytosis but not phagocytosis, was possible by using nanoparticles of polyethylene glycol [11]. Therefore, if our method can be extended to obtain cationized gelatin microspheres in the nano size range, the variety of cells to which they would be applicable may be considerably extended. It is still the case that a gene introduction method with adequate safety and efficiency for clinical application is not yet available [12]. The ingredient, gelatin, used in this study is already in clinical use, and is considered to be safe. Cationized gelatin microspheres cannot be used to introduce genes into all types of cells, and the efficiency of gene introduction is lower than that of viral vectors. However, the use of cationized gelatin microspheres to introduce a gene into endothelial progenitor cells did have an apparent and prolonged therapeutic effect [5, 6]. The smaller cationized gelatin microspheres developed in this study may provide increased efficiency of gene introduction into various cells.

In conclusion, we have improved the preparation of cationized gelatin microspheres for gene transduction, obtaining a greater yield, as well as smaller microspheres, which may have clinical potential.

ACKNOWLEDGEMENT

This work was supported by grants from Tokai University School of Medicine Research Aid in 2004 and 2005, the research and study program of Tokai University Educational System General Research Organization and Kanagawa Nanbyou foundation in 2004, as well as a Grant-in-Aid for Scientific Research in 2003 (No. 15659285) and 2005 (No. 17659375) from the Ministry of Education, Science and Culture, Japan and Health and Labour Sciences Research Grants for Research on Human Genome, Tissue Engineering Food Biotechnology in 2003 (H15-saisei-003). Health and Labour Sciences Research Grants for comprehensive Research on Cardiovascular Diseases in 2004 (H16-jyunkannki(seishuu)-009).

REFERENCES

1) Pfeifer A, Verma IM.: Gene therapy: promises and problems. Annu Rev Genomics Hum Genet 2: 177-211, 2001.
2) Kay MA, Glorioso JC, Naldini L.: Viral vectors for gene therapy: the art of turning infectious agents into vehicles of therapeutics. Nat Med 7: 33-40, 2001.
3) Ferber D.: Gene therapy. Safer and virus-free? Science 294: 1638-42, 2001.
4) Schakowski F, Buttgereit P, Mazur M, Marten A, Schottker B, Gorschluter M, Schmidt-Wolf IG.: Novel non-viral method for transfection of primary leukemia cells and cell lines. Genet Vaccines Ther 2: 1, 2004.
5) Kasahara H, Tanaka E, Fukuyama N, Sato E, Sakamoto H, Tabata Y, Ando K, Iseki H, Shinozaki Y, Kimura K, Kuwabara E, Koide S, Nakazawa H, Mori H.: Biodegradable gelatin hydrogel potentiates the angiogenic effect of fibroblast growth factor 4 plasmid in rabbit hindlimb ischemia. J Am Coll Cardiol 41: 1056-62, 2003.
6) Nagaya N, Kangawa K, Kanda M, Uematsu M, Horio T, Fukuyama N, Hino J, Harada-Shiba M, Okumura H, Tabata Y, Mochizuki N, Chiba Y, Nishioka K, Miyatake K, Asahara T, Hara H, Mori H.: Hybrid cell-gene therapy for pulmonary hypertension based on phagocytosing action of endothelial progenitor cells. Circulation 108: 889-95, 2003.
7) Cascone MG, Lazzeri L, Carmignani C, Zhu Z.: Gelatin nanoparticles produced by a simple W/O emulsion as delivery system for methotrexate. J Mater Sci Mater Med 13: 523-6, 2002.
8) Kittlick PD, Engelmann D.: The glycosaminoglycans in cultures of stimulated rat peritoneal macrophages. 2. Gel chromatographic studies and the behaviour of heparan sulfate. Exp Toxicol Pathol 45: 87-92, 1993.
9) Fukunaka Y, Iwanaga K, Morimoto K, Kakemi M, Tabata Y.: Controlled release of plasmid DNA from cationized gelatin hydrogels based on hydrogel degradation. J Control Release 80: 333-43, 2002.
10) Gedanken A.: Using sonochemistry for the fabrication of nanomaterials. Ultrason Sonochem 11: 47-55, 2004.
11) Kaul G, Amiji M.: Cellular interactions and in vitro DNA transfection studies with poly(ethylene glycol)-modified gelatin nanoparticles. J Pharm Sci 94: 184-198, 2004.
12) Tomanin R, Scarpa M.: Why do we need new gene therapy viral vectors? Characteristics, limitations and future perspectives of viral vector transduction. Curr Gene Ther 4: 357-72, 2004.
13) Rabinovich-Guilatt L, Couvreur P, Lambert G, Goldstein D, Benita S, Dubernet C.: Extensive surface studies help to analyse zeta potential data: the case of cationic emulsions. Chem Phys Lipids 131: 1-13, 2004.

Basic Res Cardiol
DOI 10.1007/s00395-■-0629-■

ORIGINAL CONTRIBUTION

Intravenous injection of phagocytes transfected ex vivo with FGF4 DNA/ biodegradable gelatin complex promotes angiogenesis in a rat myocardial ischemia/reperfusion injury model

Naoto Fukuyama
Etsuro Tanaka
Yasuhiko Tabata
Hisanori Fujikura
Masao Hagihara
Hiromi Sakamoto
Kiyoshi Ando
Hiroe Nakazawa
Hidezo Mori

Received: 18 April 2006
Returned for 1. revision: 21 June 2006
1. Revision received: 11 September 2006
Returned for 2. revision: ■
2. Revision received: ■
Accepted: 9 October 2006
Published online: ■

N. Fukuyama (✉) · H. Fujikura · M. Hagihara · K. Ando · H. Nakazawa
Depts. of Physiology, Internal Medicine and Center for Regenerative Medicine
Tokai University School of Medicine
Isehara, 259-1193, Japan
Tel.: +81-463/93-1121
Fax: +81-463/93-6684
E-Mail: fukuyama@is.icc.u-tokai.ac.jp

E. Tanaka
Dept. of Nutritional Sciences
Tokyo University of Agriculture
Tokyo, Japan

Y. Tabata
Research Center for Biomedical Engineering
Kyoto University
Kyoto, Japan

H. Sakamoto
Genetics Division
National Cancer Center Research Institute
Tokyo, Japan

H. Mori
National Cardiovascular Center Research Institute
Suita, Japan

Abstract Conventional gene therapies still present difficulties due to poor tissue-targeting, invasiveness of delivery, method, or the use of viral vectors. To establish the feasibility of using non-virally ex vivo transfected phagocytes to promote angiogenesis in ischemic myocardium, gene-transfection into isolated phagocytes was performed by culture with positively charged gelatin impregnated with plasmid DNA. A high rate of gene transfection was achieved in rat macrophages and human monocytes, but not in mouse fibroblasts. The efficiency was 68 ± 11 % in rat macrophages and 78 ± 8 % in human monocytes. Intravenously injected phagocytes accumulated predominantly in ischemic tissue (13 ± 8 %) and spleen (84 ± 6 %), but negligibly in other organs in rodents. The efficiency of accumulation in the target ischemic tissue reached more than 86 % on direct local tissue injection. In a rat model of myocardial ischemia-reperfusion, intravenous injection of fibroblast growth factor 4 (FGF4)-gene-transfected macrophages significantly increased regional blood flow in the ischemic myocardium (78 ± 7.1 % in terms of flow ratio of ischemic/non-ischemic myocardium) compared with intravenous administration of saline (36 ± 11 %) or non-transfected macrophages (42 ± 12 %), or intramuscular administration of naked DNA encoding FGF4 (75 ± 18 %). Enhanced angiogenesis in the ischemic tissue we confirmed histologically. Similarly, intravenous injection of FGF4-gene-transfected monocytes enhanced regional blood flow in an ischemic hindlimb model in mice (93 ± 22 %), being superior to the three other treatments described above (38 ± 12, 39 ± 15, and 55 ± 12 %, respectively).

Phagocytes transfected ex vivo with FGF4 DNA/gelatin promoted angiogenesis. This approach might have potential for non-viral angiogenic gene therapy.

Key words angiogenesis – cells – gene therapy – growth substances – ischemia

Abbreviations and acronyms

ANOVA = analysis of variance
FGF4 = fibroblast growth factor-4
GFP = green fluorescent protein
pI = isoelectric point

Introduction

Conventional gene therapies still require improvement with regard to transfection efficiency and safety [1, 2], as well as tissue targeting [3], despite recent advances. Achievement of a high transfection rate often requires a viral vector, but the safety of the viruses has not yet been

Basic Research in Cardiology (BRC)
Steinkopff Verlag, Darmstadt/Fotosatz Otto Gutfreund GmbH, Darmstadt
Provisional page numbers 1–8

Ms. No. BRC 629
1. run
Date 00.00.0000

BRC 629

established [4–6]. Conventional non-viral vectors seem to be inferior to viral ones in transfection efficiency, except for nucleofection [7, 8]. Conventional gene therapy using a viral vector can induce inflammation in the gene-transduced tissue [9]. Moreover, in vivo gene-delivery to the localized target tissue usually necessitates invasive approaches. For example, direct gene-transfection to cardiomyocytes requires surgical operation [10] or cardiac catheterization [11, 12]. On the other hand, ex vivo gene-transfection is less invasive, but tissue-targeting by intravenous injection is difficult to achieve [3].

Macrophages accumulate in ischemic tissue based on the mechanism of immune response (chemotaxis) [13]. This suggests that intravenous transplantation of macrophages may target the ischemic tissue in vivo. Tabata et al. previously reported that gelatin particles are phagocytized by macrophages [14, 15]. The isoelectric point (pI) of gelatin can be changed by modification of its residues, and positively charged gelatin can be impregnated with negatively charged substances [16] such as nucleic acid [17]. Thus, gelatin may be suitable as a vector for transfecting phagocytes ex vivo.

We describe here a study aimed at examining the feasibility of a new concept for less invasive, cell-based gene therapy, by means of ex vivo gene transfection into isolated phagocytes (macrophages and monocytes) using a non-viral vector, gelatin, followed by intravenous injection of the transfected phagocytes. The present method has significant advantages over conventional cell-based gene delivery [18, 19], in that the intravenously injected cells (phagocytes) not only produce protein from the transfected gene, but have a tissue-targeting ability.

Methods

This study was performed in accordance with the Guideline of Tokai University School of Medicine on Animal Use, which conforms to the NIH Guide for the Care and Use of Laboratory Animals (DHEW publication No. (NIH) 86-23, Revised 1985, Offices of Science and Health Reports, DRR/NIH, Bethesda, MD 20205).

Animals

A total of 121 Fisher rats (male, 10 weeks old, Clea Japan Inc., Tokyo) and 61 nude SCID mice (male, 6 weeks old, Shizuoka Animal Center, Shizuoka, Japan) were used. Rats were anesthetized by inhalation of diethyl ether for harvesting macrophages and with isofluren (1.5–3%) for thoracotomy, after which they were mechanically ventilated with a mixture of oxygen and nitrous oxide. Mice were anesthetized by intraperitoneal injection of sodium pentobarbital (40 mg/kg).

A model of myocardial ischemia-reperfusion injury was prepared in 41 rats. The remaining 80 rats were used for collecting activated macrophages. The heart was exposed via thoracotomy, and the proximal left anterior descending coronary artery was ligated [20] for 180 min, followed by reperfusion. A model of hindlimb ischemia was prepared in 61 mice. The left femoral artery was ligated and resected [21].

Cells

Macrophages were obtained from 80 rats. Thioglycolate (4%, 8 ml) was injected into the peritoneal cavity, and after 4 days, peritoneal macrophages were collected [22]. Monocytes were obtained from peripheral blood of healthy volunteers. Leukocyte-rich plasma was obtained by dextran 500 sedimentation and layered onto Nycoprep 1.068 (Nycomed, Birmingham, UK). The monocyte-containing layer was aspirated, washed twice and allowed to adhere to the dish for 90 minutes. Fibroblasts (NIH 3T3, Invitrogen Corporation, Carlsbad, CA) were also used. The cells were resuspended in RPMI 1640 medium (Sigma) containing 5% heat-inactivated fetal calf serum and cultured for 7–14 days. The cell viability and type were determined by trypan blue exclusion and by immunostaining using anti-macrophage antibody up to 14 days.

Genes and vector

Complementary DNA (cDNA) of green fluorescent protein (GFP), Renilla luciferase or human hst1/FGF4 (FGF4) [17] was inserted into the expression vector pRC/CMV (Invitrogen Corporation, Carlsbad, CA) and the constructs were designated as pRC/CMV-GFP, pRC/CMV-luciferase and pRC/CMV-HST1-10, respectively. Preparation and purification of the plasmid from cultures of pRC/CMV-GFP-, pRC/CMV-luciferase-, or pRC/CMV-HST1-10-transformed *Escherichia coli* were performed by equilibrium centrifugation in cesium chloride-ethidium bromide gradients.

Gelatin was prepared from porcine skin [14]. After swelling in water the gelatin particles used in this study were spheroids with a diameter of approximately 5–30 μm, water content of 95%, and pI of 11. Gelatin (2 mg) was incubated with 50 μg of the plasmid for 7 days at 4 °C to make a gelatin-DNA complex [14].

Experimental protocols

Ex vivo gene transfection Macrophages, monocytes, and fibroblasts (1×10^6) were cultured with the gelatin-DNA complex (2 mg of gelatin plus 50 μg of DNA) for 14 days on a culture dish (100 mm in diameter). Gene ex-

pression of GFP was evaluated by fluorescence microscopy and fluorescence-activated cell sorting. Luciferase activity in the cell lysate was evaluated with a photon counter system after cell lysis [23].

Organ distribution of phagocytes injected intravenously and directly into ischemic muscle To examine tissue-targeting by intravenous injection of transfected phagocytes, the distribution of the cells into organs was evaluated by immunohistochemistry. In the rat model of myocardial ischemia-reperfusion injury, the GFP-gene-transfected macrophages (1.0×10^6 each) were injected into the superficial dorsal vein of the penis at the initiation of reperfusion ($n = 7$ and 5, respectively). In the mouse model of hindlimb ischemia, the GFP-gene-transfected monocytes (1.0×10^6) were injected into the caudal vein 14 days after induction of ischemia ($n = 5$). To examine the tissue-targeting by direct local injection of transfected phagocytes, the distribution of the cells into organs was also evaluated. In the rat model of myocardial ischemia-reperfusion injury ($n = 7$) and the mouse model of hindlimb ischemia ($n = 5$), the same numbers of transfected macrophages and monocytes were directly injected into ischemic myocardium and ischemic skeletal muscle, respectively. Tissue samples were obtained 24 hours after cell administration. Each tissue was homogenized and cytospin was performed. Immunohistochemical analysis was done with anti-GFP antibody (CLONTECH, USA. GFP-monoclonal antibody). GFP positive macrophages were counted in each tissue and expressed as a percentage of total GFP-positive cells.

Amelioration of ischemia by intravenous injection of angiogenic gene-transfected phagocytes The angiogenic effect of intravenously injected FGF4-gene-transfected phagocytes on the ischemia models was evaluated. In the rat model of myocardial ischemia-reperfusion injury, FGF4-gene-transfected macrophages ($n = 5$), non-transfected macrophages (1.0×10^6 each) ($n = 5$), or saline ($n = 5$) were injected into the superficial dorsal vein of the penis, or naked FGF4-DNA (50 μg) was injected directly into the ischemic myocardium ($n = 5$), at the initiation of reperfusion. Fourteen days after the cell administration, blood flows in the ischemic and non-ischemic regions in the heart were evaluated with a non-contact laser Doppler flowmeter (FLO-N1, Omegawave Corporation). Then, tissue samples were obtained and histological analysis was performed. In a mouse model of hindlimb ischemia, just after induction of ischemia, FGF4-gene-transfected monocytes ($n = 15$), non-transfected monocytes ($n = 8$) (1.0×10^6 each), or saline ($n = 10$) were injected into the caudal vein, or naked FGF4-DNA (50 μg) was injected directly into the ischemic muscle ($n = 12$). Fourteen days after induction of ischemia, blood flows in the limbs were evaluated with the noncontact laser Doppler flowmeter (FLO-N1, Omegawave Corporation).

Histology

Ten micrometer sections were cut from formalin-fixed, paraffin-embedded tissue. Two sections were used for H.E. staining and azan staining, and eight sections were used for immunohistochemical staining. Immunohistochemical staining was performed by an indirect immunoperoxidase method. Anti-GFP antibody, anti-Mac1 antibody (BMA Biomedicals Ag, Switzerland), and anti-CD31 antibody (Serotec, UK) were used as primary antibodies. Mac1-antigen is specific to macrophages/monocytes. Anti-Ig, peroxidase-linked species-specific F(ab')2 fragments (Amersham Pharmacia Biotech UK Ltd., UK), were used as a secondary antibody. Double staining was performed with alkaline staining and peroxidase staining. The vessel density stained with von Willebrand factor-antibody was calculated by morphometric assessment in one 16 randomly selected fields of each heart and expressed as number/mm^2.

Statistical analysis

Data are presented as mean values ± SD. Differences were assessed by using ANOVA (analysis of variance) with the Scheffe's multiple comparisons test. A value of $P < 0.05$ was considered statistically significant.

Results

Ex vivo gene transfection

We studied whether genes could be transfected into isolated rat macrophages, human monocytes, and mouse fibroblasts ex vivo by using gelatin. Transfection of the GFP gene into isolated rat macrophages (Figs. 1A and B) and human monocytes (Figs. 1C and D), but not into mouse fibroblasts (data not shown), was achieved by culture with gelatin-DNA complex for 14 days. The gene transfection efficiency into rat macrophages was 68 ± 11% (30 experiments, Fig. 2A) and that into human monocytes was 78 ± 8% (30 experiments) as determined with a fluorescence activated cell sorter. Sequential analysis after luciferase-gene transfection into rat macrophages revealed high expression after 14 days of culture (Fig. 2B).

Basic Research in Cardiology
© Steinkopff Verlag 200

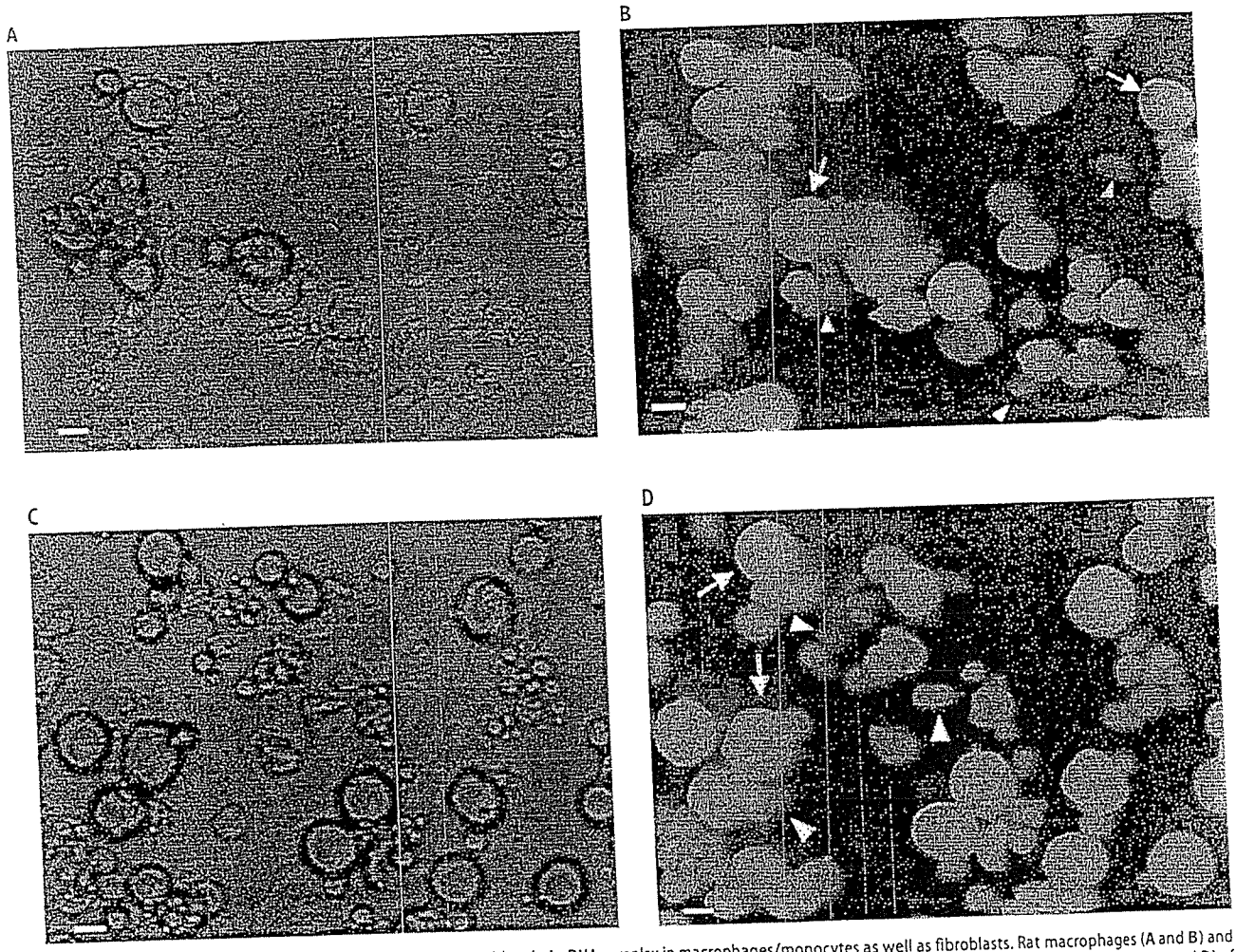

Fig. 1 Fluorescent presentation of ex vivo gene transfection with gelatin-DNA complex in macrophages/monocytes as well as fibroblasts. Rat macrophages (A and B) and human monocytes (C and D) were cultured with gelatin-GFP-gene complex for 14 days. Transmittance microscopic images (A and C) and fluorescence images (B and D) of the cells are shown. Macrophages (B) and monocytes (D) show fluorescence due to GFP. Arrowheads indicate GFP-expressing cells. Arrows indicate gelatin particles themselves. Bars = 20 μm

Organ distribution of phagocytes injected intravenously or directly into ischemic muscle

We studied quantitatively whether intravenously injected luciferase-gene-transfected phagocytes could target ischemic tissues (the third and fifth columns from the left in Table 1). In non-ischemic rats, the injected macrophages were recognized almost exclusively in the spleen (98 ± 4 %) (n = 7, the second column in Table 1). In non-ischemic mice, similar results were observed (n = 7, data not shown). In a rat with myocardial ischemia-reperfusion injury, some of the intravenously injected macrophages were incorporated into the heart (the third column in Table 1). The incorporation into the post-ischemic pericardium amounted to 13 ± 6 % (n = 7) (non-ischemic rats 0 ± 0 %, n = 7, Table 1). The incorporated cells expressed GFP (Fig. 3). Fibrosis with inflammatory infiltrates was recognized in the anterior wall of the left ventricle, extending to the interventricular septum (Figs. 3A and B). These infiltrates were mainly polymorphonuclear leukocytes and macrophages (Figs. 3C and D). Approximately 20 % of the macrophages showed GFP-positivity in this area (Figs. 3E and F). Similar tissue-targeting by intravenously injected monocytes was confirmed in a mouse model with hindlimb ischemia (13 ± 7 %, n = 7, the fifth column in Table 1). Furthermore, we studied whether local intramuscular injection increased the degree of tissue targeting (the fourth and sixth columns from the left in Table 1). After direct injection of phagocytes into ischemic muscle, 86 ± 10 % and 88 ± 6 % of the cells remained in the target tissue in the two models. Thirteen and 11 % of phagocytes in-

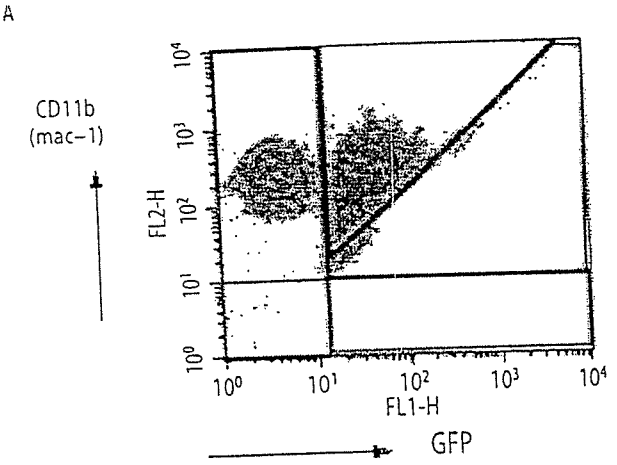

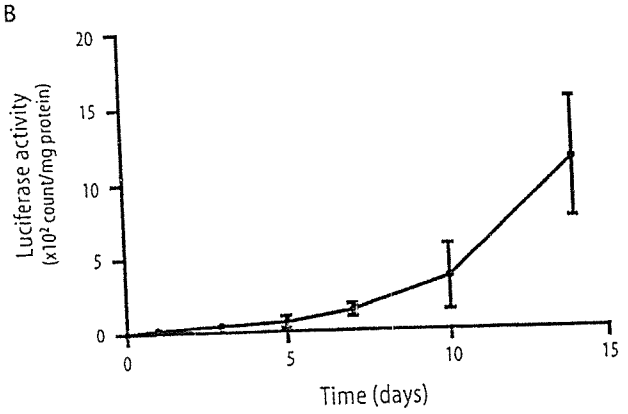

Fig. 2 Quantitative assessment of gene transfection into rat macrophages. (A) Fluorescence-activated cell sorting analysis of transfected macrophages done on day 14 of culture with reference to GFP-positive and Mac1-positive cells. (B) Sequential changes of luciferase activity in cultured macrophages in the presence of luciferase-gene-gelatin complex. Values are mean ± SD. The number of experiments is shown in parentheses

Table 1 Organ distribution of phagocytes injected into the vein and into local tissue

Organ	Normal i.v. (7 rats)	Myocardial injury i.v. (7 rats)	Myocardial injury i.m. (7 rats)	Hindlimb ischemia i.v. (7 mice)	Hindlimb ischemia i.m. (7 mice)
Heart	0±0	13±6	86±10	0±0	0±0
Hindlimb muscle	0±0	0±0	0±0	13±7	88±6
Spleen	98±4	84±6	13±10	84±6	11±6
Lung	1±2	1±1	1±2	1±2	1±1
Liver	1±2	1±1	1±1	1±2	1±1
Brain	0±0	0±0	0±0	0±0	0±0
Kidney	0±0	0±0	0±0	0±0	0±0
Intestine	0±0	0±0	0±0	0±0	0±0

Each value shows a distribution ratio (%) into organs of transfected macrophages/monocytes (mean ± SD). *i.v.* intravenous injection into the vein; *i.m.* direct injection into the jeopardized muscle

jected into the cardiac or hindlimb muscle migrated to the spleen. In the other organs, accumulation of phagocytes were negligible.

Amelioration of ischemia by intravenously injected angiogenic-gene-transfected phagocytes

In the rat model with myocardial ischemia-reperfusion injury, we studied the angiogenic effect of intravenously injected macrophages transfected with fibroblast growth factor 4 (FGF4) gene by using gelatin. Intravenous injection of these macrophages (1.0×10^6) significantly increased the regional blood flow in the ischemic myocardium (78 ± 7.1 %, n = 8, in terms of flow ratio of ischemic/non-ischemic myocardium) compared with the other three treatments ($P < 0.05$, ANOVA), that is, intravenous administration of saline (35 ± 10 %, n = 8), intramuscular administration of naked DNA encoding FGF4 (50 μg, direct intramyocardial injection after thoracotomy) (58 ± 5.3 %, n = 8), and intravenous administration of the same number of non-transfected macrophages (42 ± 12 %, n = 8) (Fig. 4A). Histological analyses revealed angiogenesis in the ischemic tissue after the administration of transfected cells (Figs. 4B and C). Similar results were observed in the mouse model with hindlimb ischemia. Intravenous injection of FGF4-gene-transfected monocytes (1.0×10^6) enhanced regional blood flow in the ischemic leg (Fig. 4D). The increase of blood flow in the mice with transfected monocytes (93 ± 22 % in terms of flow ratio of ischemic/non-ischemic leg) was significantly larger than those obtained with the other three treatments described above (38 ± 12, 55 ± 12, and 39 ± 15 %, $P < 0.05$, ANOVA). Neither lymph node swelling in any part of the body nor pathologic change in the spleen or lung, such as angioma or abnormal immune response, was found in any of the animals.

Discussion

The advantages of the present method are as follows. First, genes can easily be transfected into phagocytes (macrophages/monocytes). In preliminary experiments, we found that genes can also be transfected into endothelial progenitor cells [25]. Compared with other transfection method, the transfection efficiency was high (68 ± 11 %) and it is not necessary to use a potentially hazardous viral vector [2, 26, 32]. Second, the phagocytes can target the pathologic tissues by chemotaxis even after intravenous injection, and higher tar-

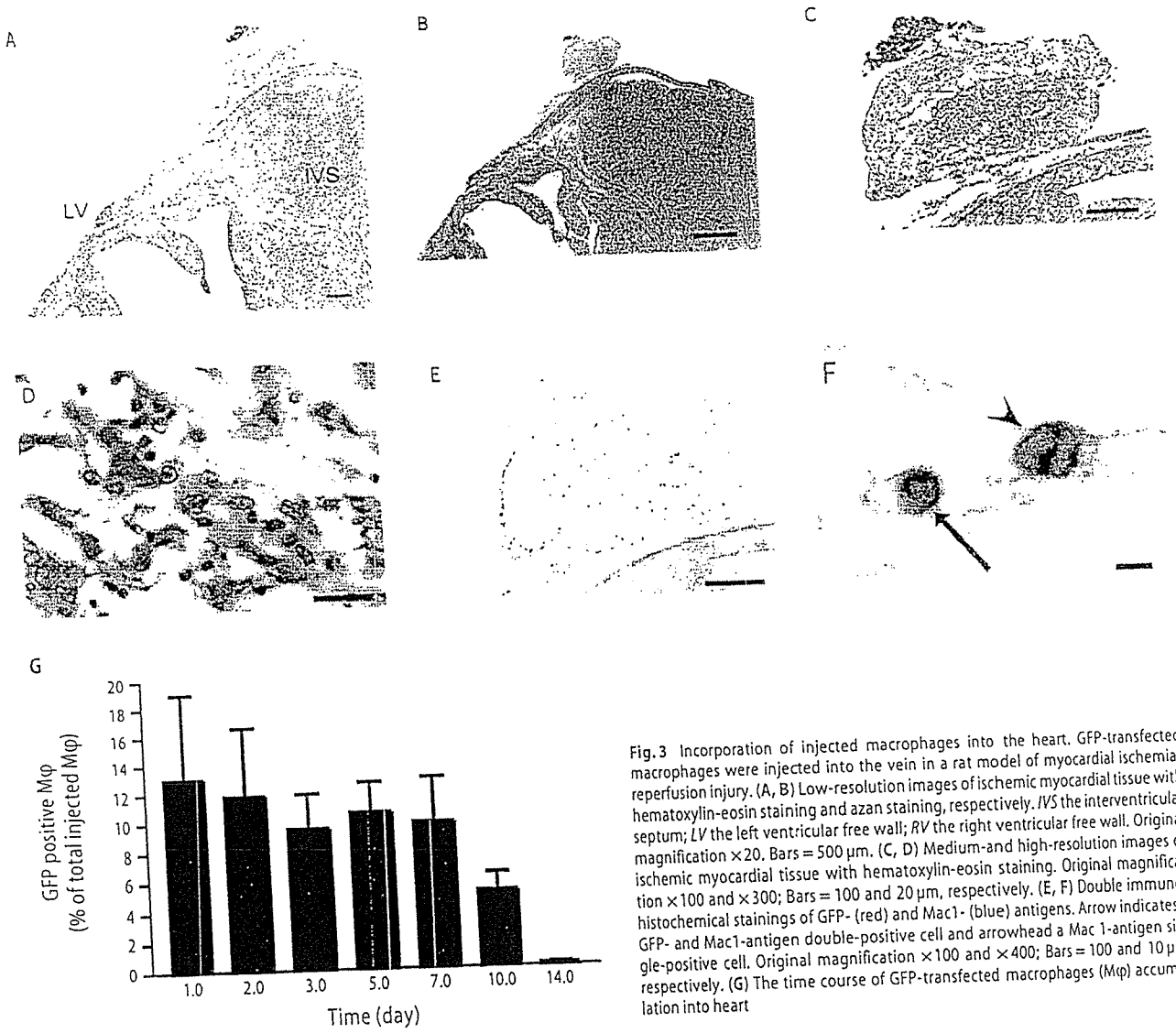

Fig. 3 Incorporation of injected macrophages into the heart. GFP-transfected macrophages were injected into the vein in a rat model of myocardial ischemia-reperfusion injury. (A, B) Low-resolution images of ischemic myocardial tissue with hematoxylin-eosin staining and azan staining, respectively. *IVS* the interventricular septum; *LV* the left ventricular free wall; *RV* the right ventricular free wall. Original magnification ×20. Bars = 500 μm. (C, D) Medium-and high-resolution images of ischemic myocardial tissue with hematoxylin-eosin staining. Original magnification ×100 and ×300; Bars = 100 and 20 μm, respectively. (E, F) Double immunohistochemical stainings of GFP- (red) and Mac1- (blue) antigens. Arrow indicates a GFP- and Mac1-antigen double-positive cell and arrowhead a Mac 1-antigen single-positive cell. Original magnification ×100 and ×400; Bars = 100 and 10 μm, respectively. (G) The time course of GFP-transfected macrophages (Mφ) accumulation into heart

geting is available if they are administered locally. The injection is repeatable. We confirmed that the angiogenic gene-transfected phagocytes enhanced angiogenesis after ischemia-reperfusion injury in rat heart and ameliorated ischemia in a mouse hindlimb model.

The injected phagocytes migrated into pathologic tissues, presumably in response to the release of cytokines such as monocyte chemoattractant protein 1 by injured endothelial cells [27]. Adhesion molecules such as P-selectin [28] are probably involved in the recruitment of phagocytes to the vessel wall. The injected phagocytes also migrated to the spleen, but no pathologic change was found in the spleen.

The present method has several advantages over conventional methods of cell-based gene therapy such as fibroblast-based and smooth muscle cell-based approaches [18, 19, 33, 34]. For example, monocytes do not aggregate in vessels, while fibroblasts or smooth muscle cells cannot be injected intravenously because of aggregation. The transfected phagocytes not only synthesize protein from the transfected gene, but also are partially targeted to the impaired tissue. In addition, the transfection rate was better than those of methods such as lipofection, viral vectors and electroporation [26, 29]. The newly developed technique of nucleofection has a transfection efficiency of 40–70% [30], which is similar to that of our method, but our procedure is easier to use [30, 31]. Further, the therapeutic effect obtained here was superior to that of conventional gene therapy which we reported previously, i.e., intramuscular injection of

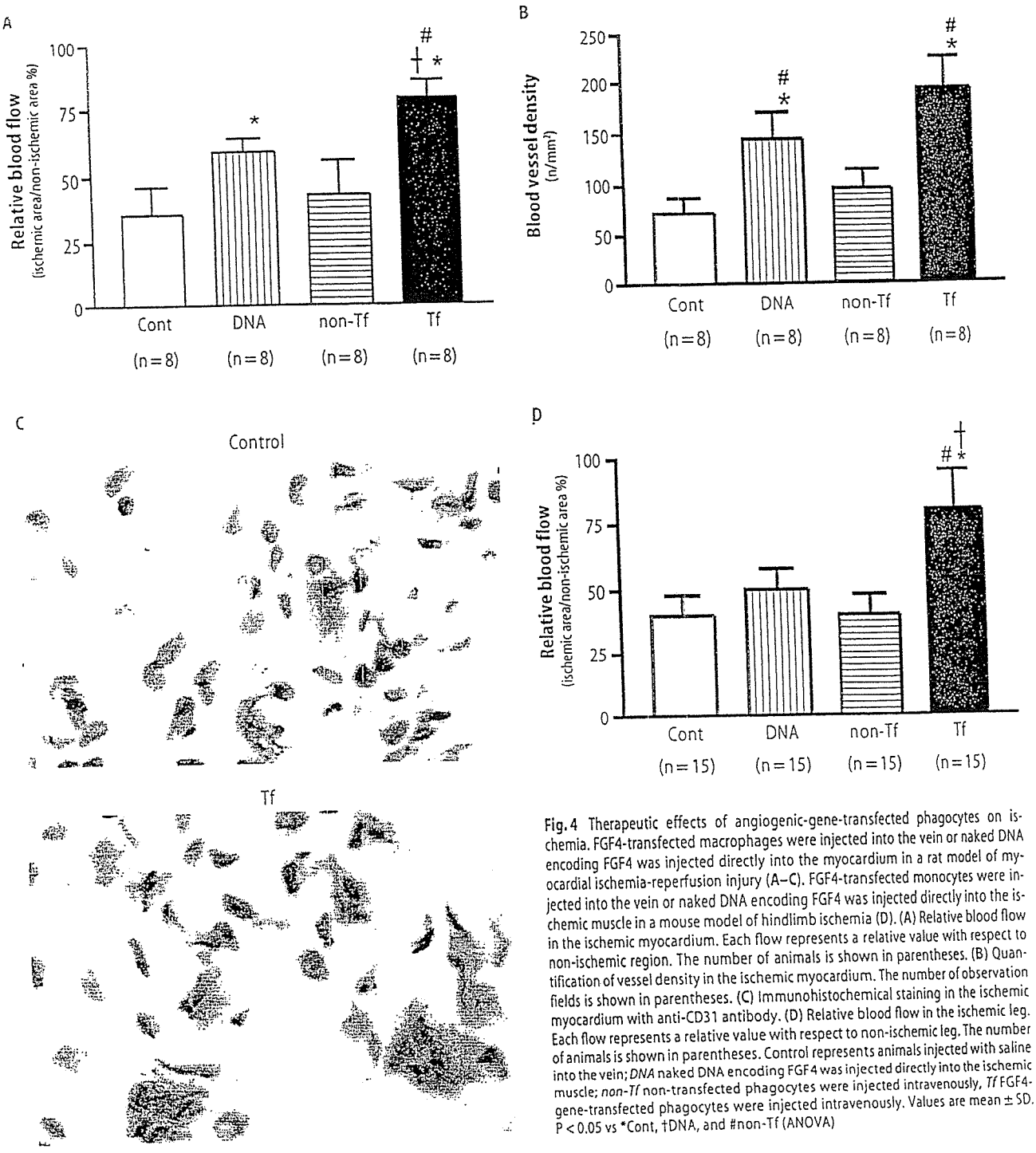

Fig. 4 Therapeutic effects of angiogenic-gene-transfected phagocytes on ischemia. FGF4-transfected macrophages were injected into the vein or naked DNA encoding FGF4 was injected directly into the myocardium in a rat model of myocardial ischemia-reperfusion injury (A–C). FGF4-transfected monocytes were injected into the vein or naked DNA encoding FGF4 was injected directly into the ischemic muscle in a mouse model of hindlimb ischemia (D). (A) Relative blood flow in the ischemic myocardium. Each flow represents a relative value with respect to non-ischemic region. The number of animals is shown in parentheses. (B) Quantification of vessel density in the ischemic myocardium. The number of observation fields is shown in parentheses. (C) Immunohistochemical staining in the ischemic myocardium with anti-CD31 antibody. (D) Relative blood flow in the ischemic leg. Each flow represents a relative value with respect to non-ischemic leg. The number of animals is shown in parentheses. Control represents animals injected with saline into the vein; *DNA* naked DNA encoding FGF4 was injected directly into the ischemic muscle; *non-Tf* non-transfected phagocytes were injected intravenously, *Tf* FGF4-gene-transfected phagocytes were injected intravenously. Values are mean ± SD. $P < 0.05$ vs *Cont, †DNA, and #non-Tf (ANOVA)

naked DNA, in ischemia models of heart and leg [17]. The major disadvantage of our method is the cell preparation time of 2 weeks before therapy can be started, and further work is needed to speed up this process.

Acknowledgements The authors wish to thank Jobu Itoh, Yoshiko Shinozaki, and Takayuki Hasegawa for their technical work.

References

1. Pfeifer A, Verma IM (2001) Gene therapy: promises and problems. Annu Rev Genomics Hum Genet 2:177–211
2. Watson DJ, Kobinger GP, Passini MA, Wilson JM, Wolfe JH (2002) Targeted transduction patterns in the mouse brain by lentivirus vectors pseudotyped with VSV, Ebola, Mokola, LCMV, or MuLV envelope proteins. Mol Ther 5:528–537
3. Li Q, Bolli R, Qiu Y, Tang XL, Guo Y, French BA (2001) Gene therapy with extracellular superoxide dismutase protects conscious rabbits against myocardial infarction. Circulation 103: 1893–1898
4. Ferber D (2001) Gene therapy. Safer and virus-free? Science 294:1638–1642
5. Kay MA, Glorioso JC, Naldini L (2001) Viral vectors for gene therapy: the art of turning infectious agents into vehicles of therapeutics. Nat Med 7:33–40
6. Isner JM (2002) Myocardial gene therapy. Nature 415:234–239
7. Nishikawa M, Hashida M (2002) Nonviral approaches satisfying various requirements for effective in vivo gene therapy. Biol Pharm Bull 25:275–283
8. Schakowski F, Buttgereit P, Mazur M, Mazur M, Marten A, Schottker B, Gorschluter M, Schmidt-Wolf IG (2004) Novel non-viral method for transfection of primary leukemia cells and cell lines. Genet Vaccines Ther 2:1
9. Tomasoni S, Benigni A (2004) Gene therapy: how to target the kidney. Promises and pitfalls. Curr Gene Ther 4: 115–122
10. Losordo DW, Vale PR, Symes JF, Dunnington CH, Esakof DD, Maysky M, Ashare AB, Lathi K, Isner JM (1998) Gene therapy for myocardial angiogenesis: initial clinical results with direct myocardial injection of phVEGF165 as sole therapy for myocardial ischemia. Circulation 98:2800–2804
11. Kornowski R, Leon MB, Fuchs S, Vodovotz Y, Flynn MA, Gordon DA, Pierre A, Kovesdi I, Keiser JA, Epstein SE (2000) Electromagnetic guidance for catheter-based transendocardial injection: a platform for intramyocardial angiogenesis therapy. Results in normal and ischemic porcine models. J Am Coll Cardiol 35:1031–1039
12. Laitinen M, Hartikainen J, Hiltunen MO, Eranen J, Kiviniemi M, Narvanen O, Makinen K, Manninen H, Syvanne M, Martin JF, Laakso M, Yla-Herttuala S (2000) Catheter-mediated vascular endothelial growth factor gene transfer to human coronary arteries after angioplasty. Hum Gene Ther 11:263–270
13. Ramsay SC, Weiller C, Myers R, Cremer JE, Luthra SK, Lammertsma AA, Frackowiak RS (1992) Monitoring by PET of macrophage accumulation in brain after ischaemic stroke. Lancet 339:1054–1055
14. Tabata Y, Ikada Y (1987) Macrophage activation through phagocytosis of muramyl dipeptide encapsulated in gelatin microspheres. J Pharm Pharmacol 39: 698–704
15. Tabata Y, Ikada Y (1988) Macrophage phagocytosis of biodegradable microspheres composed of L-lactic acid/glycolic acid homo- and copolymers. J Biomed Mater Res 22:837–858
16. Ikada Y, Tabata Y (1998) Protein release from gelatin matrices. Adv Drug Deliv Rev 31:287–301
17. Kasahara H, Tanaka E, Fukuyama N, Sato E, Sakamoto H, Tabata Y, Ando K, Iseki H, Shinozaki Y, Kimura K, Kuwabara E, Koide S, Nakazawa H, Mori H (2003) Biodegradable gelatin hydrogel potentiates the angiogenic effect of fibroblast growth factor 4 plasmid in rabbit hindlimb ischemia. J Am Coll Cardiol 41:1056–1062
18. Xie Y, Yang ST, Kniss DA (2001) Three-dimensional cell-scaffold constructs promote efficient gene transfection: implications for cell-based gene therapy. Tissue Eng 7:585–598
19. Panetta CJ, Miyauchi K, Berry D, Simari RD, Holmes DR, Schwartz RS, Caplice NM (2002) A tissue-engineered stent for cell-based vascular gene transfer. Hum Gene Ther 13:433–441
20. Gidh-Jain M, Huang B, Jain P, el-Sherif N (1996) Differential expression of voltage-gated K+ channel genes in left ventricular remodeled myocardium after experimental myocardial infarction. Circ Res 79:669–675
21. Takeshita S, Zheng LP, Brogi E, Kearney M, Pu LQ, Bunting S, Ferrara N, Symes JF, Isner JM (1994) Therapeutic angiogenesis. A single intraarterial bolus of vascular endothelial growth factor augments revascularization in a rabbit ischemic hind limb model. J Clin Invest 93:662–670
22. Ribeiro RA, Flores CA, Cunha FQ, Ferreira SH (1991) IL-8 causes in vivo neutrophil migration by a cell-dependent mechanism. Immunology 73:472–477
23. Fukuyama N, Ichimori K, Su Z, Ishida H, Nakazawa H (1996) Peroxynitrite formation from activated human leukocytes. Biochem Biophys Res Commun 224:414–419
24. Mori H, Haruyama S, Shinozaki Y, Okino H, Iida A, Takanashi R, Sakuma I, Husseini WK, Payne BD, Hoffman JI (1992) New nonradioactive microspheres and more sensitive X-ray fluorescence to measure regional blood flow. Am J Physiol 263:H1946–H1957
25. Nagaya N, Kangawa K, Kanda M, Uematsu M, Horio T, Fukuyama N, Hino J, Harada-Shiba M, Okumura H, Tabata Y, Mochizuki N, Chiba Y, Nishioka K, Miyatake K, Asahara T, Hara H, Mori H (2003) Hybrid cell-gene therapy for pulmonary hypertension based on phagocytosing action of endothelial progenitor cells. Circulation 108: 889–895
26. Kobinger GP, Deng S, Louboutin JP, Vatamaniuk M, Matschinsky F, Markmann JF, Raper SE, Wilson JM (2004) Transduction of human islets with pseudotyped lentiviral vectors. Hum Gene Ther 15:211–219
27. Leonard EJ, Yoshimura T (1990) Human monocyte chemoattractant protein-1 (MCP-1). Immunol Today 11:97–101
28. Ikeda Y, Young LH, Lefer AM (2002) Attenuation of neutrophil-mediated myocardial ischemia-reperfusion injury by a calpain inhibitor. Am J Physiol Heart Circ Physiol 282:H1421–H1426
29. Veit K, Boissel JP, Buerke M, Grosser T, Meyer J, Darius H (1999) Highly efficient liposome-mediated gene transfer of inducible nitric oxide synthase in vivo and in vitro in vascular smooth muscle cells. Cardiovasc Res 43:808–822
30. Maasho K, Marusina A, Reynolds NM, Coligan JE, Borrego F (2004) Efficient gene transfer into the human natural killer cell line, NKL, using the Amaxa nucleofection system. J Immunol Methods 284:133–140
31. Mertz KD, Weisheit G, Schilling K, Luers GH (2002) Electroporation of primary neural cultures: a simple method for directed gene transfer in vitro. Histochem Cell Biol 118:501–506
32. Lei Y, Haider HK, Shujia J, Sim ES (2004) Therapeutic angiogenesis; Devising new strategies based on past experiences. Basic Res Cardiol 99:121–132
33. Ott HC, McCue J, Taylor DA (2005) Cell-based cardiovascular repair: The hurdles and the opportunities. Basic Res Cardiol 100:504–517
34. Koch KC, Schaefer WM, Liehn EA, Rammos C, Mueller D, Schroeder J, Dimassi T, Stopinski T, Weber C (2006) Effect of catheter-based transendocardial delivery of stromal cell-derived factor 1α on left ventricular function and perfusion in a porcine model of myocardial infarction. Basic Res Cardiol 101:69–77

Tokai J Exp Clin Med., Vol. 31, No. 3, pp. 128-132, 2006

Search for appropriate experimental methods to create stable hind-limb ischemia in mouse

Takako GOTO[*1], Naoto FUKUYAMA[*2], Akira AKI[*1], Kazuo KANABUCHI[*1], Koji KIMURA[*1], Hiroyuki TAIRA[*1], Etsuro TANAKA[*5], Noriaki WAKANA[*3], Hidezo MORI[*4] and Hiroshi INOUE[*1]

*Departments of [*1] Surgery and [*2] Physiology, Tokai University School of Medicine*
*[*3] Department of Nutritional Sciences, Tokyo University of Agriculture, Tokyo, Japan*
*[*4] Department of Cardiac Physiology, National Cardiovascular Center Research Institute, Suita, Japan*

(Received June 26, 2006; Accepted July 19, 2006)

***Objective*:** Stable animal models for refractory peripheral arterial disease are not established. A standardized animal model of hind-limb ischemia is required upon searching effective treatment for this condition. The aim of the study is to verify previously used hind-limb ischemia models to find a standard method.
***Methods*:** Using Balb/ca mice six various methods of inducing hind-limb ischemia were applied and two weeks after operation degree of ischemic damage were examined. Six methods include V group, A group, AV group, A-strip group, AV-strip group and Prox-A group (refer the text).
***Results*:** Degree of ischemia was evaluated macroscopically by judging toes, foot, knee, and total hind-limb necrosis. We found that severity of damage was markedly different among different methods. Furthermore the severity of necrosis was not uniform even in the same method group.
***Conclusions*:** The A-strip group in which the femoral artery from the bifurcation of the deep femoral artery to the saphenous artery was stripped appears to be suitable as a stable severe ischemia model. The A group in which the femoral artery were cut just below the bifurcation of the deep femoral artery appears to be suitable as a chronic mild ischemia model.

Key words: angiogenesis, animal model, blood vessels, femoral artery, hind-limb ischemia

INTRODUCTION

Refractory peripheral arterial disease is becoming an important therapeutic target since its incidence has been markedly increasing due to the increase in aged population and patients with diabetes mellitus. Consequently various therapeutic approaches including angiogenic treatment with growth factors or cell transplantation have been attempted using mouse hind-limb ischemia models [1-4]. Scrutinizing these studies we found that experimental methods to create hind-limb ischemia are not standardized. Method of occluding artery varies from ligation, or cutting, to excision of the artery. The targeted artery varies also from the iliac artery [1], the femoral artery [2-4], or the femoral with saphenous artery [5-9]. In some cases, both the femoral artery and vein were occluded. Strangling of the thigh itself was attempted in some studies [10, 11]. As the severity of ischemic damage cannot be uniform in different experimental methods, the comparison of effect among various therapies becomes very difficult.

Another important problem in previously used animal models is lack of data on blood flow when hind-limb is lost. In case of severe ischemic damage in mouse necrosis and loss of hind-limb often occur within three days but in patients of peripheral artery disease ischemia is chronic and acute necrosis is seldom seen. In these patients the improvement of blood flow is one of the key indices in determining effective treatments. Therefore it is mandatory to have an animal model in which chronic hind-limb ischemia is present but necrosis seldom occurs and sequential evaluation of blood flows is possible in order to evaluate various therapies.

In the present study, firstly we examined six methods for inducing hind-limb ischemia in Balb/ca mice and evaluated the severity of ischemic change to search for a stable severe ischemia model. Secondly we selected three methods with mild ischemic changes among six methods which do not produce severe necrosis and examined degree of ischemia by measuring CPK release, muscle weight, and histological changes to find an appropriate mild ischemia model.

MATERIALS AND METHODS

Animals

Seventy-five male Balb/ca mice (12 weeks old, 20 to 30 g, Japan Clea Inc, Ishibe) were used. All operations and measurements were performed under general anesthesia (1.0 to 1.5% isoflurane, 60% dinitrous monoxide, and 40% oxygen). The operation was performed, by only one investigator (T.G.), under a microscope (Konan Operation Microscope 707, Konan Keeler Co. LTD, Japan). To create ischemia, the vessels were cut or resected after ligation of the stumps with sterilized 6-0 silk suture (Azwel Inc, Osaka). The investigation conforms with The Guide for the Care and Use of Laboratory Animals published by the U.S. National Institutes of Health (NIH Publication No. 85-23, revised 1996).

Takako GOTO, Department of Surgery, Tokai University School of Medicine, Isehara, Kanagawa 259-1193, Japan Tel: 0463-93-1121 ext:2280 Fax: 0463-95-7567
E-mail: gotoh-ta@is.icc.u-tokai.ac.jp

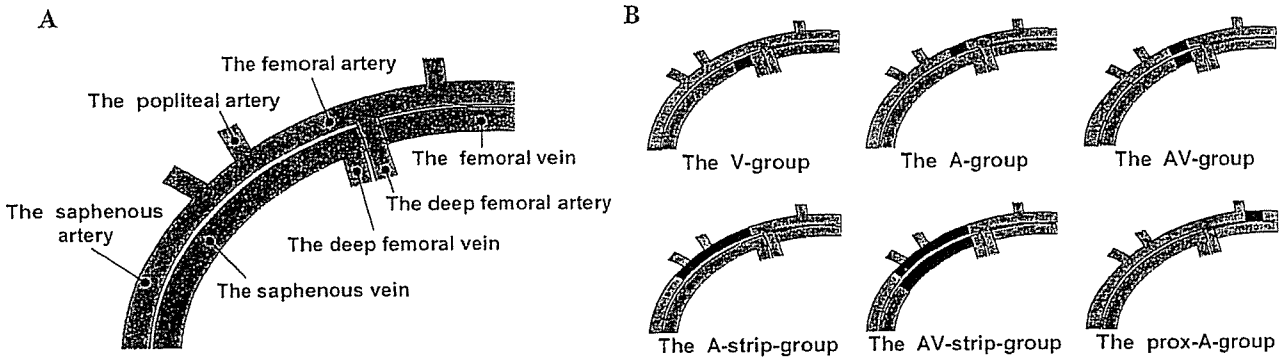

Fig. 1 (A) Schematic illustration of vascular anatomy in the mouse lower limb. (B) Schematic illustrations of surgical procedures in the six groups. The black bar indicates the cut or stripped sites of the vessels.

EXPERIMENTAL PROTOCOLS

1. The six hind limb ischemia models (n = 60)

The following six types of ischemia were created in the right lower limbs of 60 mice (schematic illustrations are presented in Fig. 1). These included, (1) cutting the femoral vein at the distal site of the bifurcation of the deep femoral vein (V-group, n = 10), (2) cutting the femoral artery just below the bifurcation of the deep femoral artery (A-group, n = 10), (3) cutting both the femoral artery and vein (AV-group, n = 10), (4) resection of the femoral artery from the distal site of the bifurcation of the deep femoral artery to the saphenous artery (A-strip-group, n = 10). By disecting the femoral artery as was shown in the Fig. 1B, branches including the popliteal artery were also obstracted and retrograde flows from these branches were completely avoidable. (5) resecting both the femoral artery and vein from the distal site of the bifurcation of the deep femoral artery to the saphenous artery (AV-strip-group, n = 10), and (6) cutting the femoral artery at the proximal site of the bifurcation of the deep femoral artery (Prox-A-group, n = 10).

2. Macroscopic evaluation of ischemic severity

Two weeks after the operation, the ischemic limb was macroscopically evaluated by using graded morphological scales for necrotic area; grade 0: absence of necrosis, grade I: necrosis limiting to toes (toes loss), grade II: necrosis extending to a dorsum pedis (foot loss), grade III: necrosis extending to a crus (knee loss), grade IV: necrosis extending to a thigh (total hind-limb loss).

3. Blood flow measurement

Calf blood flows on both sides were measured below a patella with a noncontact laser Doppler flowmeter (FLO-N1, Omegawave Corporation, Tokyo) before the operation, just after the operation, and two weeks post operatively, and were expressed as the ratio of the flow in the ischemic limb to that in the normal limb.

4. CPK release, muscle weights and histological evaluation in three mild ischemia groups

In additional mice of V-, A-, and AV-groups (n = 5 each) blood samples were obtained from the orbital plexus before the operation and 1, 2, and 7 days thereafter and concentrations of creatine phosphokinase (CPK) were measured. At two weeks after the operation, the animals were sacrificed under an overdose of sodium pentobarbital and the anterotibial, gastrocnemius, and soleus muscles were dissected out and weighed. Histological analysis (HE staining) was performed in each muscle [12].

Table 1 Degree of Ischemic Damage in 6 Groups.

Group \ Grade	0	I	II	III	IV
V group	10				
A group	7	3			
AV group	5	5			
A-strip-group	1	9			
AV-strip-group		6	3	1	
Prox-A-group		3			7

0: no change, I: toes necrosis, II: foot necrosis,
III: knee necrosis, IV: total necrosis

RESULTS

1) Severity of ischemic change in the six groups

Two weeks after the operation necrotic changes were macroscopically evaluated (Table 1). In the V-group, no macroscopic change was observed throughout the experimental period. In other 5 groups tissue necrosis appeared at either toes, dorsum pedis, crus or thigh. The position of necrosis was not uniform even in one group. Loss of total hind-limb was observed only in the Prox-A-group (7/10 mice). The order of necrosis severity among groups were Prox-A-group, AV-strip-group, A-strip-group, AV-group and A-group. The necrosis occurred as early as three days after the operation when it happens.

2) Changes in calf blood flow in the six groups

Just after the operation, calf blood flows were decreased to 30-35% of the pre-operative value without significant differences among the six groups except for the V-group (V-group: 98.5 ± 1.7, A-group: 34.1 ± 12.8, AV-group, 34.4 ± 9.9, A-strip-group: 31.4 ± 3.6, AV-strip-group: 32.9 ± 5.0 and Prox-A-group: 31.3 ±

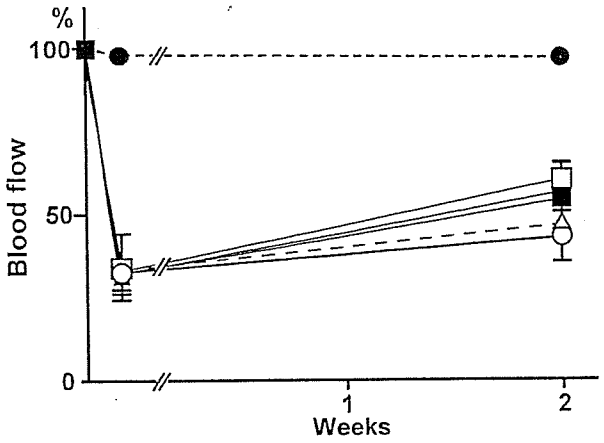

Fig. 2 Blood flow changes in 6 groups. Blood flow is express as a ratio of that in the ischemic limb to that in the opposite limb. V-group: closed circles, A-group: open circles, AV-group: open triangles, A-strip-group: closed triangles, AV-strip group: open squares, Prox-A-group: closed squares. Measurement of blood flows was available only in intact hind-limb or in stable data in case of toes necrosis.

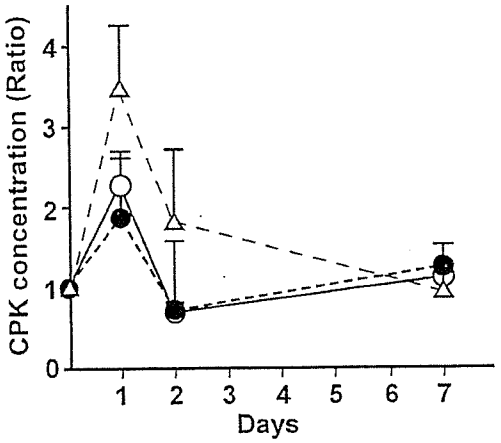

Fig. 3 Concentrations of serum creatine phosphokinase (CPK) in three groups. The concentration is expressed as the value relative to that before the operation. V-group: closed circles, A-group: open circles, AV-group: open triangles.

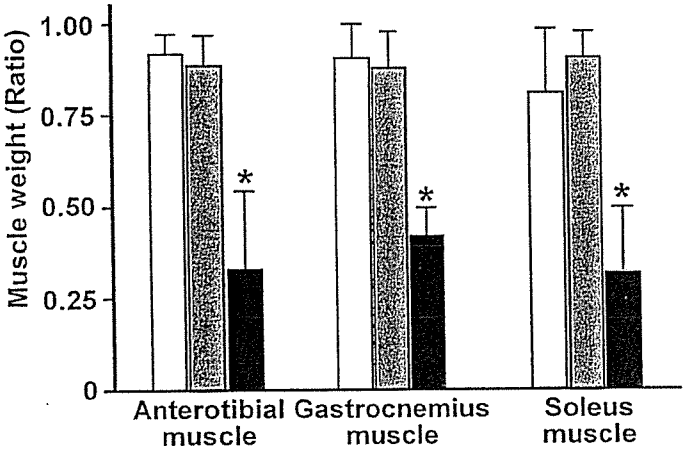

Fig. 4 Muscle weights in the ischemic limb at 14 days after the operation. The weights of the three muscles are expressed as the value relative to those of the same muscles in the opposite limb. V-group: open bar, A-group: grey bar, AV-group: black bar. ($p<0.05$ vs A- and V-groups, ANOVA).

6.5%, respectively, Fig. 2). Two weeks after the operation, calf blood flows had recovered to 45-55% of the pre-operative value (V-group: 97.8 ± 1.2, A-group: 44.7 ± 8.9, AV-group, 48.0 ± 9.0, A-strip-group: 54.0 ± 6.2, AV-strip-group: 57.0 ± 7.3 and Prox-A-group: 59.8 ± 5.1, respectively). The blood flow measurement was applicable only in mice in which calf was well preserved. We found difficulty to obtain stable calf blood flow in some mice with toes necrosis even though their calf was preserved and unstable measurements were omitted. Namely blood flow could be measured in 10 mice in the V group, 10 mice in the A group, 8 mice in the AV-group, 8 mice in the A-strip-group, 7 mice in the AV-strip-group, 3 mice in the Prox-A-group. At two weeks there were no significant differences among the six groups except for the V-group.

3) CPK release, muscle weights and histological evaluation in three mild ischemia groups

As we found that ischemic changes were too severe in A-strips, AV-strip and Prox-A-groups, we selected V-, A- and AV-groups as mild ischemia models. Blood CPK concentrations were significantly elevated one day after the operation in V-, A- and AV-groups ($p<0.05$ vs pre-operation, ANOVA, Fig. 3). Two days after the operation, CPK values had returned to baseline in the A- and V-groups but were still high in the AV-group ($p<0.05$ vs pre-operation, ANOVA). Seven days after the operation, CPK values had returned to baseline in all groups.

Two weeks after the operation, weight loss in the calf muscles was observed only in the AV-group. The values relative to those of the same muscles in the opposite limb were anterotibial: 0.32 ± 0.22, gastrocnemius: 0.42 ± 0.08, and soleus muscles: 0.32 ± 1.8 (Fig. 4). HE staining of the gastrocnemius muscle in the V-group disclosed that there was not obvious changes in the V-group compared with that in the normal limb (Figs. 5A and B). On the other hand, in the A- and AV-groups, microscopic features of necrotic changes such as cell size inhomogeneity, cellular wall degeneration, denucleation, and edema were observed (Figs. 5C

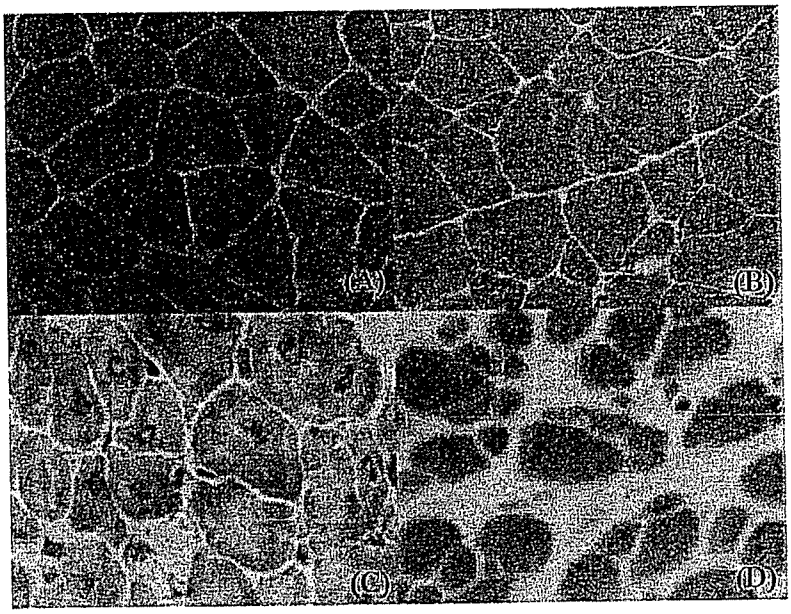

Fig. 5 There was not obvious changes in the V-group compared with that in the normal limb. In the A- and AV-groups, microscopic features of necrotic changes such as cell size inhomogeneity, cellular wall degeneration, denucleation, and edema were observed.

and D). These changes were more severe in the AV-group than in the A-group.

DISCUSSION

The mouse hind-limb has a well-developed innate collateral system and is shown to have remarkably high resistance to ischemia, e.g., a simple ligation of the femoral artery is known to produce no serve ischemic change [1]. This is because the hind-limb would be nourished by collateral circulation via the deep femoral artery and other branches (Fig. 1). As was shown in the Fig. 1A, there are several small branches including the popliteal artery and simple ligation of the femoral artery (A-group) results in obstruction of forward flow, but collateral flows via the deep femoral artery from these branches can retrogradely enter the distal portion of the femoral artery. In contrast, when the site of ligation is proximal, the deep femoral arterial flow will be also interrupted. Similarly in the A-strip group collateral flows from branches cannot enter the distal portion of the femoral artery. When site of ligation is proximal or includes several branches, collateral flow reduces and ischemic change becomes severe. However degree of ischemic damage would not be the same even in the site of ligation because richness and course of collateral vessels differ markedly among individual animals.

As was expected, this study revealed that the degree of ischemic damage varies markedly in six models of mouse hind-limb ischemia. Another important finding of this study is that even in the one model the ischemic damages were not uniform ranging from toes necrosis to knee necrosis as such in the AV-strip-group or from toes necrosis to total hind-limb necrosis in the Prox-A-group (Table 1). Only the A-strip-group showed relatively uniform ischemic damage: 9 toes necrosis and one no change.

On examining effect of various therapies including angiogenic treatments with growth factors or cell transplantation we have to use stable and uniform ischemic damage model, but previous studies used various degree of ischemic damage [1-9]. In this study we showed that A-strip method appears to be most appropriate as a mild ischemia model. The Prox-A method can be utilized when very severe ischemic damage model is necessary.

Regarding mild ischemia model simple ligation of the vein without treatment of the artery (V-group in protocol 2, Fig. 5B) produced only very weak edematous change and this is not an ischemic model. However, obstruction of venous return appears to have additional effects because damage became more serious in the AV-group than that in the A-group (Table 1 and Fig. 5). For example, edematous changes were seen by the histological analysis in the AV-group, and the AV-group showed muscle weight reduction in all anterotibial, gastrocnemius and soleus muscles (Fig. 5). Since venous obstruction is not associated with peripheral arterial disease, pathology under AV-group cannot be consistent with patients suffering from peripheral arterial disease. Although blood flow measurements were possible in both A- and AV-groups, severity of ischemic damage was relatively stable in the A-group, which resembles to the degree of ischemia seen in patients (7 mice showed no necrosis and three had toes necrosis). Taken together, the A-group appears to be the most suitable as a chronic mild ischemia model.

In conclusion, the relatively severe stable ischemia model is created by stripping the femoral artery from the distal site of the bifurcation of the deep femoral artery to the saphenous artery and the mild ischemic model should be made by cutting the femoral artery